NATIONAL ADVISORY COMMITTEE FOR AERONAUTICS

TECHNICAL NOTE 3763

NEAR NOISE FIELD OF A JET-ENGINE EXHAUST

I - SOUND PRESSURES

By Walton L. Howes and Harold R. Mull

Lewis Flight Propulsion Laboratory
Cleveland, Ohio

Washington
October 1956

NATIONAL ADVISORY COMMITTEE FOR AERONAUTICS

TECHNICAL NOTE 3763

NEAR NOISE FIELD OF A JET-ENGINE EXHAUST

I - SOUND PRESSURES

By Walton L. Howes and Harold R. Mull

SUMMARY

The acoustical near field produced by the exhaust of a stationary turbojet engine having a high pressure ratio was measured for a single operating condition without afterburning. The maximum over-all sound pressure without afterburning was found to be about 42 pounds per square foot along the jet boundary in the region immediately downstream of the jet-nozzle exit. With afterburning the maximum sound pressure was increased by 50 percent. The largest sound pressures without afterburning were obtained in the frequency range from 350 to 700 cps.

Additional tests were made at a few points to find the effect of jet velocity on near-field sound pressures and to determine the difference in value between sound-pressure levels at rigid surfaces and corresponding free-field values. Near the jet nozzle, over-all sound pressures were found to vary as a low power (approx. unity) of the jet velocity. Over-all sound-pressure levels considerably greater than the corresponding free-field levels were recorded at the surface of a rigid plate placed along the jet boundary.

The downstream locations of the maximum sound pressure at any given frequency along the jet-engine-exhaust boundary and the longitudinal turbulent-velocity maximum of the same frequency along a small cold-air jet at 1 nozzle-exit radius from the jet axis were found to be nearly the same when compared on a dimensionless basis. Also, the Strouhal number of the corresponding spectra maximums was found to be nearly equal at similar distances downstream.

INTRODUCTION

Experience has shown that jet-induced acoustical pressures, particularly in the immediate vicinity of the exhaust of a jet engine, can be of sufficient magnitudes to cause fatigue failure of adjacent surfaces. Moreover, these near-field sound pressures may produce harmful effects on ground and flight personnel if they are not shielded from the noise.

The acoustical near field is a loosely defined region immediately surrounding any multipole source of sound or distribution of multipole sources. Specifically, any point whose distance from an acoustical source is not large compared with the acoustical wavelength is said to be within the near field of the source. In the acoustical near field, sound pressures are not in phase with sound particle velocities.

Present knowledge of magnitudes and spectra of near-field jet noise from turbojet engines is quite limited. Data on the acoustical near field of air jets are reported in references 1 and 2. Noise surveys about jet engines are presented in references 3 and 4. The data on engine noise have been limited generally to distances greater than 10 feet from the jet-nozzle exit.

Jet-noise abatement at the source is the most desirable method for solving the structural and personnel problems. Knowledge of the space distribution of acoustical sources as to type, orientation, size, intensity, and frequency is important in connection with the noise-abatement problem. Ultimately, a complete theory of jet noise is desired.

Any complete theoretical analysis of the jet as a noise source should be capable of predicting the sound pressures, spectra, and pressure correlations in space and time throughout the noise field. Lighthill has developed a basic theory of aerodynamic noise (ref. 5) and, subsequently, has extended this theory (ref. 6) to explain the production of sound by jets for the subsonic regime. According to this theory, jet turbulence, particularly in regions of large mean shear (e.g., in the jet-mixing region), is a source of sound. In general, the jet can be subdivided into small volumes, which may be regarded as individual sources of sound. Each source is represented mathematically as an acoustical quadrupole, that is, a high-order source composed of four simple poles. Experimental measurements have borne out the more general predictions of Lighthill's theory. However, before any complete theory of jet noise can be confirmed, additional experimental data are required. Near-field jet noise represents one phase of the over-all problem that merits experimental investigation, not only to provide data for further theoretical development, but also to provide data relating to the structural problem.

This report contains results of a survey of near-field sound-pressure levels and spectra in the vicinity of the jet produced by a stationary axial-flow turbojet engine having a high pressure ratio across the jet nozzle. The measurements were obtained as part of a study of jet noise at the NACA Lewis laboratory. The corresponding sound-pressure correlations are presented in reference 7. The data reported herein extend to within a few inches of the jet-nozzle exit and

jet boundary. Except for ground effects, the results of this report are associated with free-field conditions. Some additional acoustical data obtained at the surface of a stiff plate, and with afterburning are also included.

APPARATUS

The jet-noise measurements described in this report were obtained from the axial-flow turbojet engine shown in figure 1. This engine is rated at more than 10,000 pounds of sea-level static thrust and has a circular convergent nozzle. The engine was mounted with its centerline 6 feet above ground level in the thrust stand also shown in figure 1.

A 12-foot-high sound-absorbent wall composed of acoustical panels comprised the only large obstacle near the field of measurement. The wall was erected early in the program in order to reduce noise levels within the nearest buildings, which were about 1/10 mile forward of the engine. It was quite unlikely that the presence of the wall could affect noise levels in the field of measurement.

A block diagram of the sound analyzing equipment is shown in figure 2. The acoustical pickup consisted of a small condenser microphone and included preamplifier. The output from this unit is linear at all sound-pressure levels less than 180 decibels. (Sound-pressure level in decibels in this report is based on a reference pressure of 2×10^{-4} dyne/cm^2 and has a frequency response that is flat to within 1 decibel from 35 to 8000 cps.) Corrections for microphone response were applied to data for frequencies greater than 3000 cps. Power for the unit was obtained from a separate power supply. The output passed through a frequency-compensated cable to a 1/3-octave-band audiofrequency spectrometer and automatic recorder, which were located in a control room approximately 150 feet from the field of measurement. The power supply was kept in an acoustically treated box (fig. 3) in order to prevent its destruction by the intense noise. The useful frequency range of the entire unit was 35 to 15,000 cps. The entire system was calibrated with a 400-cps signal supplied by a small calibrator loudspeaker driven by a transistor oscillator.

Sound-pressure levels were recorded in decibels. The recorded levels do not correspond to intensity levels because of the arbitrary phase relation between the sound-pressure and particle-velocity fluctuations in the acoustical near field.

The microphone unit was mounted on an extension arm from a remote-controlled motor-driven probe actuator. In addition, a second identical microphone was fixed at one end of the actuator support (fig. 3) for obtaining data at two points during short runs (e.g., during

afterburning). The actuator allowed the microphone to be located at several points without stopping the engine. Successive positions of the microphone were remotely indicated within the control room. The actuator permitted a maximum linear traverse of the microphone of 8 feet without moving the actuator itself. The support was provided with various adjustments to permit the microphone to be kept in the horizontal plane containing the engine axis when the actuator was located over uneven ground.

PROCEDURE

The jet velocity and temperature profiles in the horizontal plane containing the engine axis were measured first in order to locate the jet boundary, that is, to determine how near the microphone could be brought to the jet without being affected by jet gusts or overheating. A string grid was laid out along the ground in order to locate points in the noise field.

Measured jet velocity and temperature boundaries for the fixed operating condition without afterburning are indicated in figure 4. In figure 4, abscissa values represent distances along the jet axis measured from the jet-nozzle exit. Ordinate values represent radial distances measured perpendicular to the jet axis and in the horizontal plane containing the jet axis. Indicated boundary values correspond to measurement stations at which average total pressures (velocity boundary) and average total temperatures were found to be within 0.05 inch of mercury and 5° F, respectively, of the ambient values. The solid line in figure 4 corresponds to the boundary of the noise measurements; that is, no noise measurements were made at stations corresponding to points below the solid line in figure 4. The boundary of the noise measurements was constructed at a slightly greater azimuth than those of the velocity and temperature boundaries in order to minimize the impingement of jet gusts upon the microphone in the presence of cross-winds. In particular, the boundary azimuth values measured with respect to the jet axis were as follows:

(1) Velocity boundary, $\sim 6.7^{\circ}$

(2) Temperature boundary, $\sim 9.4^{\circ}$

(3) Boundary of noise measurements, $\sim 9.8^{\circ}$

Maps showing all points at which noise data were obtained comprise figure 5. The acoustical instrumentation was calibrated before each set of measurements.

The complete noise-field survey program extended over a period of several months. Engine operation was limited by poor weather conditions and the relative immobility of the microphone with respect to the size of the field to be surveyed. Therefore, repeatability of engine operating conditions was important for obtaining a complete field survey at a fixed operating condition.

Only one engine control variable is independent during static engine operation. Of the control variables, thrust, rotor speed, turbine-outlet temperature, and engine pressure ratio, measured engine thrust was selected as a convenient measure of repeatability. Engine thrust and the total acoustical power generated by turbulence (ref. 5) both depend upon ambient temperature and pressure, but to a different degree. Thus, constant engine thrust does not correspond to constant generated total acoustical power if ambient conditions change. Therefore, the effects of changes in ambient temperature and pressure on the measured sound field were necessarily regarded as uncorrectible errors.

The selected value of thrust and corresponding values of other significant parameters were as follows:

Thrust, lb	9600
Jet velocity, ft/sec	1850
Nozzle pressure ratio	2.2
Nozzle temperature ratio	2.8
Nozzle-exit diameter, ft	1.85

The jet velocity (a bulk velocity) was computed by dividing the measured value of thrust by the measured mass flow of gas through the engine. Good agreement between experimental data (ref. 8) and Lighthill's theoretical estimate (ref. 5) of the functional dependence of total acoustic power has been obtained by defining jet velocity in the preceding manner. The preceding values were repeatable for the entire range of ambient conditions encountered. The standard deviation of thrust and jet velocity resulting from all causes was about 1 percent and 20 feet per second, respectively.

In addition to the acoustical near-field survey at a fixed operating condition, measurements were made at a few points for various jet velocities without and with afterburning. Also, a few acoustical measurements were made at the surface of a stiff plate placed along the jet boundary in order to obtain an estimate of the increase of sound-pressure levels at rigid surfaces over the corresponding free-field values. The measurements at the plate surface were made for the same engine operating conditions listed previously. With afterburning the values of the significant engine parameters were as follows:

Thrust, lb	14,750
Jet velocity, ft/sec	2,590
Nozzle-exit diameter, ft	2.33

Variations of experimental conditions resulted principally from wind, ambient temperature and pressure variations, and mislocation of the microphone. Tests were restricted to days on which wind velocities were less than 15 mph in order to minimize the influence of wind on the jet as a noise source. Accurate positioning of the microphone is particularly important in regions of large sound-pressure gradients. The microphone was located with respect to the nozzle exit to within 1 or 2 inches and was pointed directly at (normal to) the jet axis. The microphone height was set to within 1/4 inch of the horizontal plane containing the engine axis.

RESULTS

Contour maps showing regions of equal sound-pressure levels in the acoustical near-field are presented in figures 6 and 7. The contour numbers denote (approx.) root-mean-square sound-pressure levels in decibels and are associated with an average engine thrust of 9600 pounds. The contours in figure 6 represent lines of constant over-all sound-pressure level that, for the tests described, included all frequencies between 35 and 15,000 cps. Corresponding maps for each 1/3-octave band in the frequency range from 35 to 11,200 cps are presented in figure 7. Figure 8 is provided as a convenience for comparing sound-pressure levels in decibels with sound pressures in pounds per square foot.

Free-field sound-pressure-level contours are shown in figures 6 and 7. Sound-pressure levels at surfaces may be considerably higher. For example, results presented in reference 2 and the additional tests performed using the engine described herein have revealed sound-pressure levels at the surface of a stiff plate that are considerably higher than the corresponding free-field values. As shown in figure 5(b), the present plate tests were made at two stations along the jet boundary. At the upstream station, sound-pressure levels at the plate surface were found to be 2 or 3 decibels higher than the corresponding free-field values. However, at the downstream station, the increase was found to be as much as 16 decibels, probably resulting from impingement of the jet on the plate.

Over-All Sound Pressure

The measured maximum free-field over-all sound-pressure level without afterburning was approximately 160 decibels, which corresponds to a sound pressure of 42 pounds per square foot. This sound pressure was measured along the jet boundary from 1/2 to (at least) 2 nozzle-exit diameters from the nozzle exit (fig. 6). With afterburning the maximum sound-pressure level, determined from measurements at only two stations (fig. 5(c)) along the jet boundary, was found to be 163.5 decibels at

the upstream station. This level corresponds to a sound pressure of 63 pounds per square foot. At the downstream station the level was 160 decibels.

Henceforth, considering only the free-field results without afterburning, the variation of over-all sound pressure along the jet boundary is shown in figure 9. The maximum sound pressure indicated in figure 9 is less than that indicated in figure 6 because of variations in experimental conditions, principally the ambient wind. Sound pressure, rather than sound-pressure level, was selected as the ordinate in figure 9 because sound pressure is probably more nearly proportional to acoustical-source strength within the jet.

According to figure 9, the over-all sound pressure along the boundary was a maximum up to 4 diameters downstream of the nozzle exit, fell rapidly between 4 and 25 diameters downstream, and ceased to fall rapidly beyond 25 diameters downstream. Beyond this point, the sound-pressure level was at least 20 decibels below the maximum level.

The direction of maximum sound propagation was estimated from figure 6 to form an angle between 30° and 40° with respect to the jet axis. The point of maximum sound-pressure level, rather than the center of the nozzle exit, was used as the vertex in forming this angle. This result is in agreement with the results of far-field measurements (refs. 4 and 8). The reason for the apparent curvature of the direction of maximum propagation has not been determined.

The effect of jet velocity on over-all sound pressures at various points along the jet boundary is shown in figure 10. Lighthill's theory and experimental results (ref. 9) indicate that the relation between the acoustical pressure p at a point and the jet velocity U is $p_2/p_1 = (U_2/U_1)^n$, where 1 and 2 correspond to two different values of U. Lines corresponding to various values of n are shown in figure 10. Near the nozzle $n < 1$, whereas beyond 15 diameters downstream $n \rightarrow 4$, which is approximately the value expected in the far field (refs. 5 and 6). Further experiments covering a wider range of velocities are required to establish accurately the variation of near-field sound pressures with jet velocity.

Sound-Pressure Level in Frequency Bands

The maximum sound-pressure level in any single 1/3-octave band was found to be about 150 decibels, which corresponds to a sound pressure of 13 pounds per square foot, in the three 1/3 octaves included in the interval from 350 to 700 cps. These levels were measured along the jet boundary from a point near the nozzle exit to 5.5 nozzle diameters downstream of the nozzle exit (figs. 7(k), (l), and (m)).

The distribution along the jet boundary of the sound pressure in each frequency band was found to be useful for estimating the predominant location of acoustical sources of any given frequency. The apparent location of sources in a selected frequency band was assumed to be at the same distance downstream as the maximum of the corresponding sound-pressure distribution curve. The frequency of acoustical sources as a function of distance downstream is denoted by the solid curve in figure 11(a). The dashed lines signify locations at which the sound-pressure level falls 6 decibels below the maximum level for the particular frequency. A portion of the same curve is shown in figure 11(b) with the distance downstream expressed on a logarithmic scale. Throughout most of the length of the jet-mixing region, the relation between frequency of acoustical sources and distance downstream is found from figure 11(b) to be $x^{3/4}f = 10^3$, where x is the distance downstream of the nozzle exit in feet and f is the frequency of the source in cps.

The angle of maximum sound propagation was found from the acoustical maps in figure 7 to increase with increasing frequency from about 20° at 40 cps to 45° at 10,000 cps. The variation of angle of maximum propagation as a function of frequency is shown in figure 12.

Sound-Pressure-Level Spectra Along Jet Boundary

The sound field for particular frequency bands was considered in the preceding section. The same data are now reconsidered in terms of sound-pressure-level spectra at particular field points.

Spectra along the jet boundary from approximately 1/2 to 33 nozzle-exit diameters (0.83 to 61.8 ft) downstream of the nozzle exit are presented in figure 13. Each spectrum possesses a single peak in the audible frequency range. The variation of the frequency of peak sound-pressure level as a function of axial distance from the nozzle exit is shown in figure 14. The peak frequency was considered to correspond to the frequency at the intersection of the straight lines fitting the low and high frequency fall-off portions of the spectra in figure 13. Throughout the length of the mixing region the relation between peak frequency and distance downstream of the nozzle exit is found from figure 14 to be $x^{1/2}f = 10^3$. This result does not agree with the expression given in the preceding section for locating acoustical sources because the sound pressure is not equally distributed over all the frequency bands.

Up to about 3.5 nozzle-exit diameters downstream of the nozzle exit, the spectrum sound pressures fall off at the rate of 25 decibels per frequency decade on the low-frequency end and 15 decibels per decade on the high-frequency end (fig. 13). Beyond 5 diameters downstream of the

nozzle exit, the low-frequency fall-off rate decreases to 15 or 20 decibels per decade, whereas the high-frequency fall-off rate remains unchanged.

Second-Source Noise

Profiles of sound-pressure levels along the jet boundary for each frequency band and the acoustical maps in figure 7 indicate the possible existence of a wide-frequency-band noise source in the vicinity of the jet-nozzle exit. Along the jet boundary this "second-source" noise is differentiable from the jet-induced noise only at frequencies less than 100 cps, as shown, for example, in figure 15. Moreover, the presence of secondary lobes in the acoustical maps (fig. 7) also indicates the existence of a second noise source. It seems likely that the second-source noise is either shock-produced noise or internally generated engine noise that is propagated out of the engine tailpipe. The operational engine pressure ratio (2.2) is identical to that associated with the onset of shock-induced noise from small air jets (refs. 1 and 10). However, the maximum acoustical pressures at any frequency which are attributable to the second source are appreciably less than those caused by the jet turbulence alone.

DISCUSSION

The results concerned with direction of maximum sound propagation, its variation with frequency, and the trend of the distribution according to frequency of acoustical sources along the jet are in general agreement with those presented in references 1 and 4. However, noise levels reported herein are considerably higher than the levels reported in reference 4, especially in regions nearest the jet nozzle. On the other hand, the present noise levels agree with the engine noise levels reported in reference 2.

Unfortunately, previously published data on the acoustical near field of jets are insufficient to permit comparison with the present results to more than a very limited extent. However, a considerable amount of jet-turbulence data for an unheated-air jet issuing from a circular convergent nozzle is given in reference 11. Comparing the air-jet turbulence data in reference 11 with the jet-engine acoustical data is of interest in attempting to relate jet-engine sound fields to those of air jets and in relating turbulence to sound. Two comparisons were made:

(1) Comparison of the distance downstream of root-mean-square sound-pressure and longitudinal turbulent-velocity maximums for each 1/3-octave band

(2) Comparison of the frequencies of the sound-pressure-spectrum and longitudinal turbulent-velocity-spectrum maximums as a function of distance downstream

The values of the significant parameters associated with the air-jet turbulence data in reference 11 are

Jet velocity, ft/sec	342
Nozzle pressure ratio	1.06
Nozzle temperature ratio	1.01
Nozzle-exit diameter, in.	3.5

Because these values differed greatly from those associated with the engine acoustical data, the preceding comparisons were made, as suggested by the work of Lighthill and Greatrex, on the basis of Strouhal number (based on jet bulk velocity and nozzle-exit diam.) rather than frequency, and distances downstream were expressed in jet-nozzle-exit diameters. The comparisons were made between noise measured along the jet boundary and turbulence measured along the jet length at a distance of 1 nozzle-exit radius from the jet axis. At distances less than 20 nozzle-exit diameters downstream of the nozzle exit the over-all longitudinal turbulent-velocity fluctuations are a maximum at about 1 nozzle-exit radius from the jet axis (refs. 11 and 12).

The results of the comparisons are presented in figures 16 and 17. In figure 16, the Strouhal numbers of the sound-pressure and longitudinal turbulent-velocity maximums are plotted as a function of distance downstream of the nozzle exit in nozzle-exit diameters. A similar plot which locates the frequencies of the corresponding spectra maximums is shown in figure 17. The acoustical and turbulence spectra (in terms of Strouhal number, rather than frequency) at corresponding dimensionless distances downstream are compared in figure 18.

The good agreement between the curves for sound and turbulence in figure 16 is appreciably better than that which resulted when frequency, rather than Strouhal number, was adopted as the ordinate. The present result indicates that, at least in the mixing region, frequencies of turbulent-velocity fluctuations are associated with noise of the same frequency. (The same conclusion is reached in ref. 13 from theoretical considerations.) Moreover, the distribution according to frequency of acoustical sources in the air jet was similar to that in the jet-engine exhaust. The distribution was relatively independent of jet temperature. Peak noise and turbulence at frequencies corresponding to values of Strouhal number larger than 0.15 occurred upstream of the tip of the jet core ($x/d < 4.5$, where d is the nozzle-exit diam. and x is distance downstream from nozzle exit), that is, in the jet-mixing region.

The acoustical and turbulence spectra in figure 18 are nearly identical at a point near the nozzle, but the turbulence spectra tend to be flatter than the corrresponding acoustical spectra downstream of the nozzle. As shown in figure 17, the maximum of the acoustical spectra varies less as a function of distance downstream than does the corresponding maximum of the turbulent-velocity spectra. The effect amounts to stretching, in the flow direction, the jet-flow field of the engine with respect to that of the air jet. The effect is not one of temperature because the velocity field of a jet becomes compressed longitudinally as the jet temperature is increased (see figs. 7 and 10 of ref. 14). Rather, choking of the jet, which commences at a nozzle pressure ratio of 1.89, appears to explain the stretching of the engine flow field. In the presence of choking, the rate of expansion of the mixing region is less than for unchoked conditions (ref. 15).

Comparing the downstream distance of the acoustical and turbulence maximums for a given frequency is not the same as comparing the frequency of the corresponding spectra maximums at the same distance downstream of the nozzle exit, because the maximum level and spectrum maximum for a given frequency may not occur at the same distance downstream. Comparisons of the frequencies of spectra maximums at the same distance downstream are made in references 11 and 16. However, comparing the locations of the maximum levels associated with a given frequency (fig. 16) is more directly related to locating acoustical sources according to frequency.

Although the maximum over-all turbulence occurs at about 1 nozzle-exit radius from the jet axis, the maximum turbulence at a specified frequency may not occur at 1 nozzle-exit radius. Therefore, the entire field of turbulence should be taken into account in determining the location of the turbulence maximum for a given frequency. In comparing this location with the acoustical results, the distance of the turbulence maximum from the jet boundary should also be considered. In the present comparisons, the two preceding effects were disregarded.

CONCLUSIONS

Acoustical measurements in the vicinity of the exhaust of a 10,000-pound-static-thrust turbojet engine indicated that:

1. Maximum over-all root-mean-square pressures were of the order of 42 pounds per square foot without afterburning or 63 pounds per square foot with afterburning. These pressures correspond to sound-pressure levels of 160 and 163.5 decibels, respectively. Maximum sound pressures were obtained along the jet boundary immediately downstream of the jet-nozzle exit.

2. Maximum sound pressures of the order of 13 pounds per square foot occurred (without afterburning) in each of the three 1/3-octave bands contained in the frequency interval from 350 to 700 cps.

3. Sound-pressure levels at the surface of a stiff plate placed along the jet boundary were found to be considerably greater than the corresponding free-field values.

4. Throughout most of the length of the jet-mixing region, the distribution according to frequency of acoustical sources was given by $x^{3/4}f = 10^3$, where x is the distance downstream of the nozzle exit in feet and f is the frequency of the source in cps.

5. Throughout the length of the mixing region, the relation between spectrum peak frequency and distance downstream was given by $x^{1/2}f = 10^3$, where x and f are defined in the preceding result.

By comparing the acoustical measurements for the engine with turbulence measurements for a cold-air jet, the following additional conclusions appear valid:

1. Peak longitudinal turbulent velocities and peak acoustical pressures associated with the same Strouhal number occur at approximately the same dimensionless distance along a jet.

2. Peak longitudinal turbulent velocities and peak acoustical pressures at approximately the same dimensionless distance along a jet possess the same Strouhal number.

3. The distribution according to frequency of acoustical sources along the hot exhaust of a jet engine is similar to that along a cold-air jet. The effect of jet temperature upon the distribution appears to be small or negligible. The rate of expansion of the jet-mixing region may affect the distribution.

4. Acoustical spectra adjacent to a jet-engine exhaust are similar to, but not as flat as, longitudinal turbulent-velocity spectra at 1 nozzle-exit radius and at a similar distance along an air jet.

5. Acoustical and turbulent-velocity frequencies corresponding to values of Strouhal number larger than 0.15 are generated primarily in the jet-mixing region upstream of the tip of the jet core.

The preceding conclusions resulted when the acoustical and turbulence data were compared in terms of distance downstream in jet-nozzle-exit diameters and Strouhal number based on jet-nozzle-exit diameter and the jet bulk velocity.

Lewis Flight Propulsion Laboratory
National Advisory Committee for Aeronautics
Cleveland, Ohio, May 10, 1956

4009

REFERENCES

1. Westley, R., and Lilley, G. M.: An Investigation of the Noise Field from a Small Jet and Methods for Its Reduction. Rep. No. 53, The College of Aero. (Cranfield), Jan. 1952.

2. Lassiter, Leslie W., and Hubbard, Harvey H.: The Near Noise Field of Static Jets and Some Model Studies of Devices for Noise Reduction. NACA TN 3187, 1954.

3. Greatrex, F. B.: Engine Noise. Joint Symposium on Aero. Acoustics (London), May 21, 1953.

4. Greatrex, F. B.: Jet Noise. Preprint No. 559. Inst. Aero. Sci., June 1955.

5. Lighthill, M. J.: On Sound Generated Aerodynamically. I. General Theory. Proc. Roy. Soc. (London), ser. A, vol. 211, no. 1107, Mar. 20, 1952, pp. 564-587.

6. Lighthill, M. J.: On Sound Generated Aerodynamically. II. Turbulence as a Source of Sound. Proc. Roy. Soc. (London), ser. A, vol. 222, no. 1148, Feb. 23, 1954, pp. 1-32.

7. Callaghan, Edmund E., Howes, Walton L., and Coles, Willard D.: Near Noise Field of a Jet-Engine Exhaust. II - Cross Correlation of Sound Pressures. NACA TN 3764, 1956.

8. Coles, Willard D., and Callaghan, Edmund E.: Investigation of Far Noise Field of Jets. II - Comparison of Air Jets and Jet Engines. NACA TN 3591, 1956.

9. Lassiter, Leslie W., and Hubbard, Harvey H.: Experimental Studies of Noise from Subsonic Jets in Still Air. NACA TN 2757, 1952.

10. Callaghan, Edmund E., and Coles, Willard D.: Investigation of Far Noise Field of Jets. I - Effect of Nozzle Shape. NACA TN 3590, 1956.

11. Laurence, James C.: Intensity, Scale, and Spectra of Turbulence in Mixing Region of Free Subsonic Jet. NACA TN 3561, 1955.

12. Laurence, James C., and Stickney, Truman M.: Further Measurements of Intensity, Scale, and Spectra of Turbulence in a Subsonic Jet. NACA TN 3576, 1956.

13. Mawardi, Osman K.: On the Spectrum of Noise from Turbulence. Jour. Acoustic Soc. Am., vol. 27, no. 3, May 1955, pp. 442-445.

14. Corrsin, Stanley, and Uberoi, Mahinder S.: Further Experiments on the Flow and Heat Transfer in a Heated Turbulent Air Jet. NACA Rep. 998, 1950. (Supersedes NACA TN 1865.)

15. Gooderum, Paul B., Wood, George P., and Brevoort, Maurice J.: Investigation with an Interferometer of the Turbulent Mixing of a Free Supersonic Jet. NACA Rep. 963, 1950. (Supersedes NACA TN 1857.)

16. Hubbard, H. H., and Lassiter, L. W.: Experimental Studies of Jet Noise. Jour. Acoustic Soc. Am., vol. 25, no. 3, May 1953, pp. 381-384.

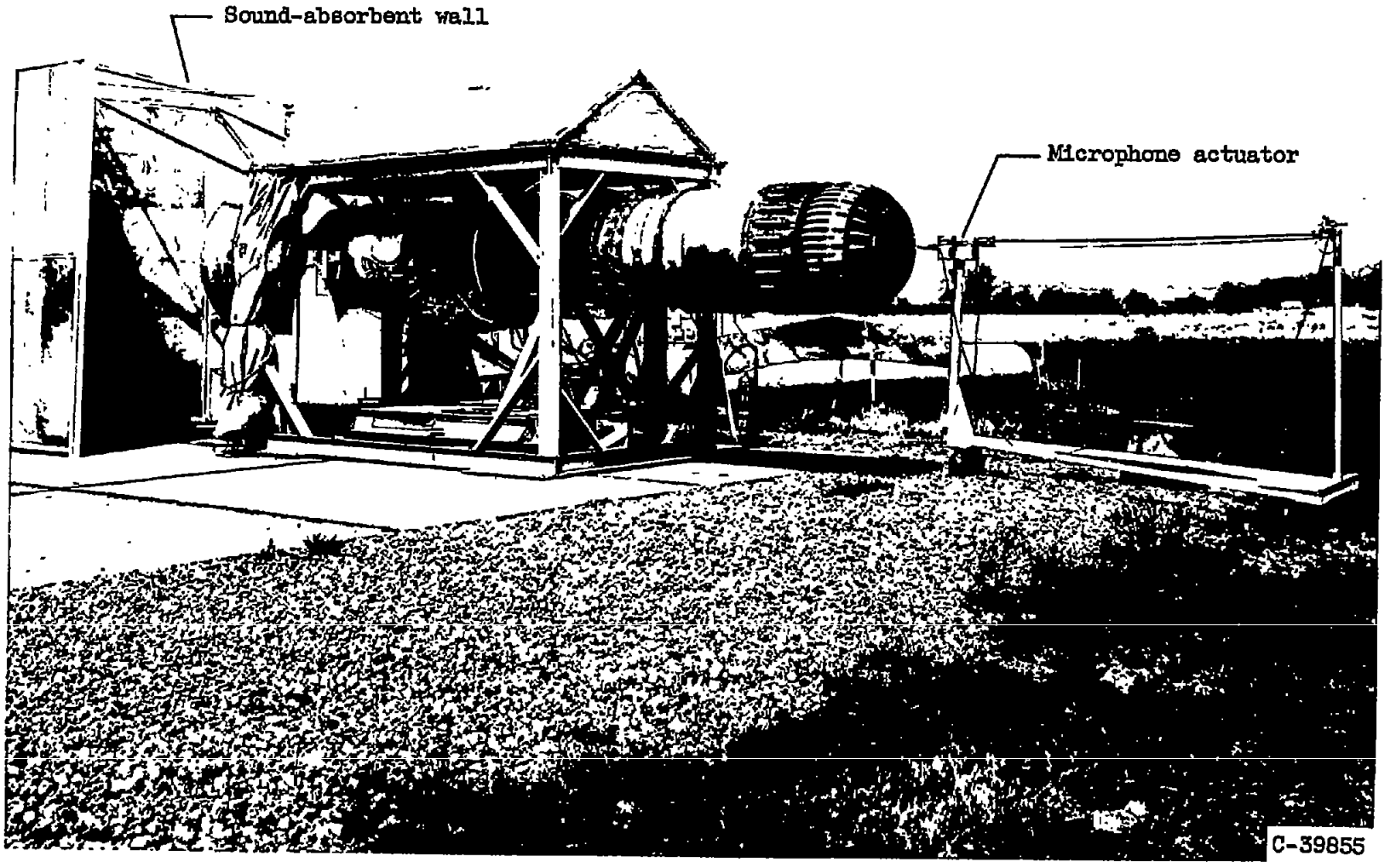

Figure 1. - Engine installation and microphone actuator.

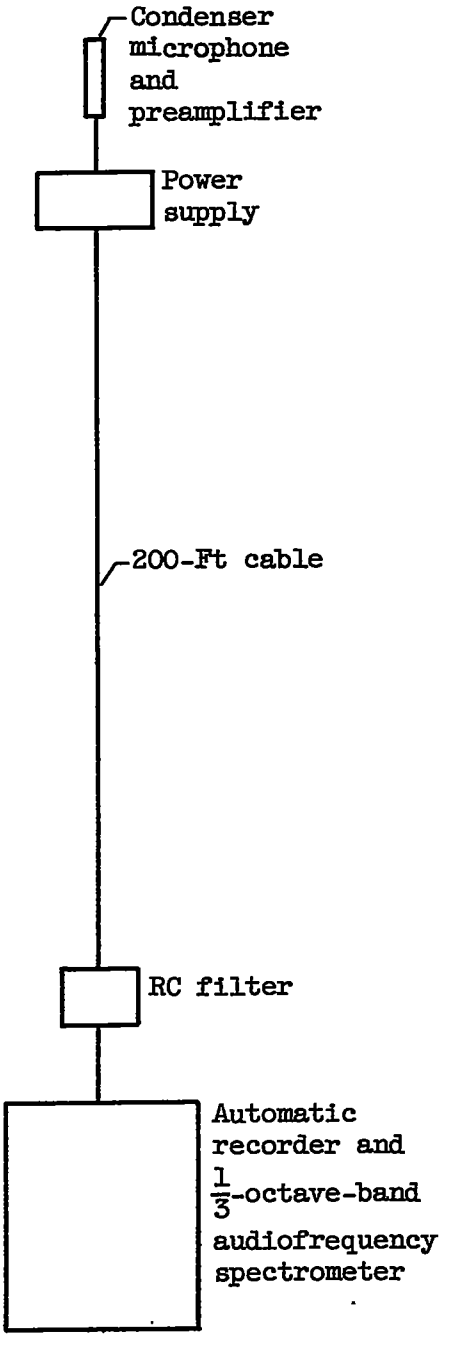

Figure 2. - Sound analyzing equipment.

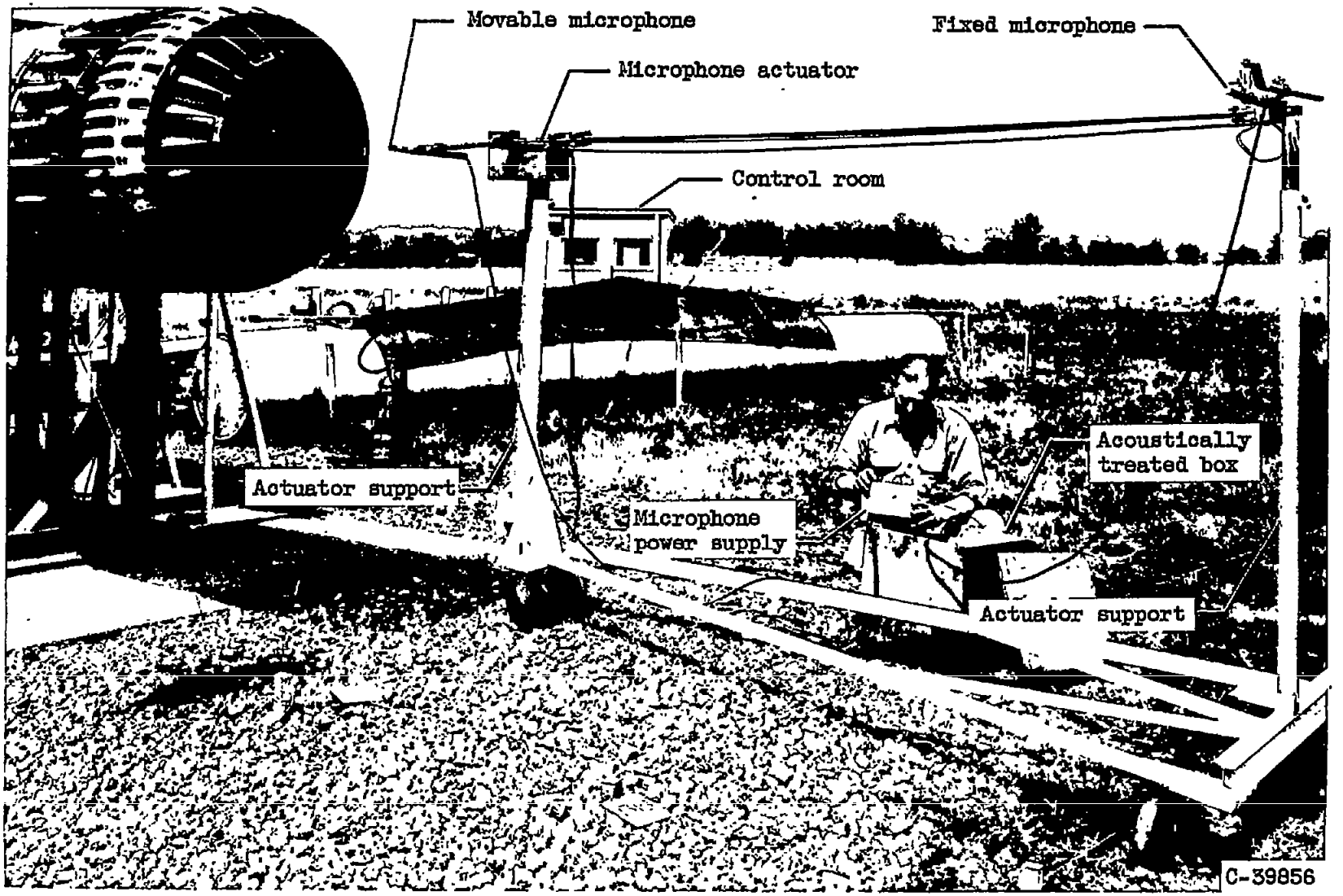

Figure 3. - Microphone actuator and support.

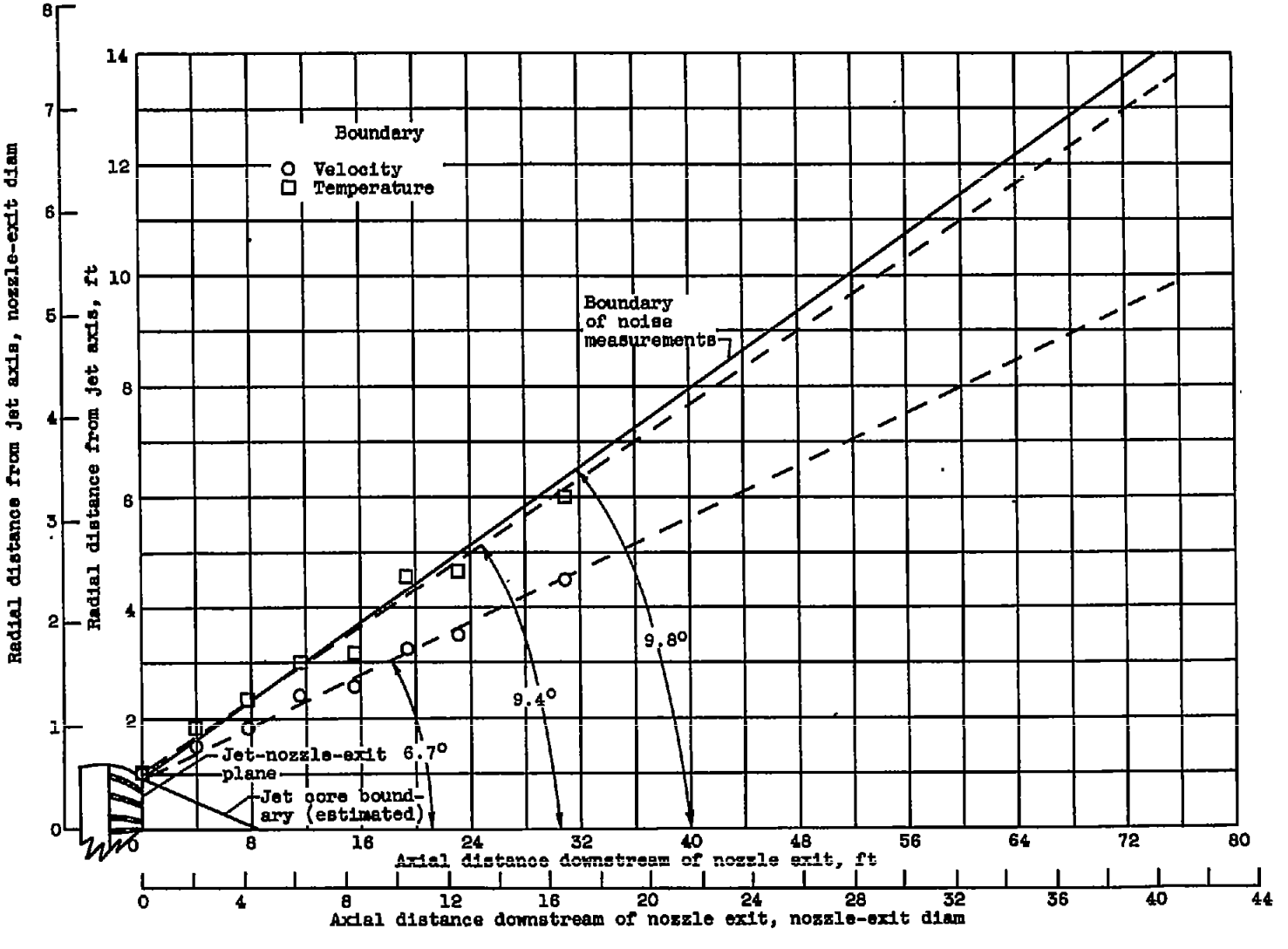

Figure 4. - Locus of jet velocity, temperature, and acoustical measurement boundaries.

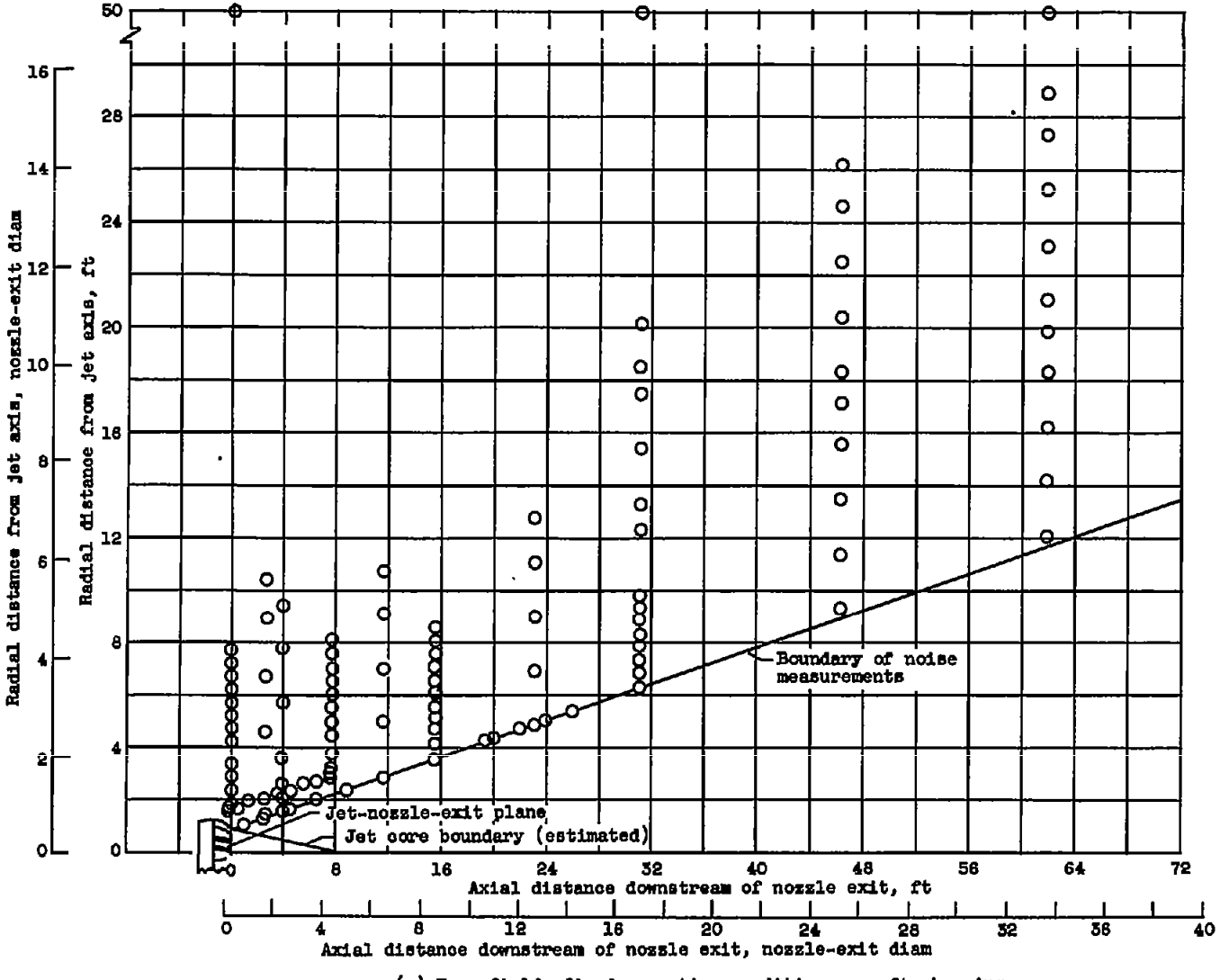

(a) Free field, fixed operating condition; nonafterburning.

Figure 5. - Locus of near-field-noise measurements.

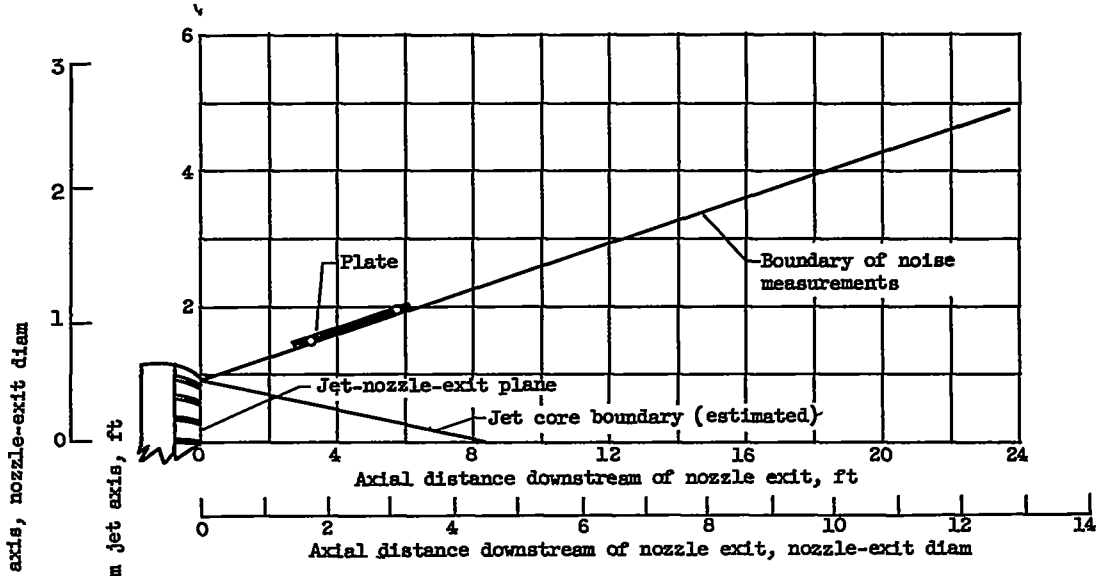

(b) At plate surface; nonafterburning.

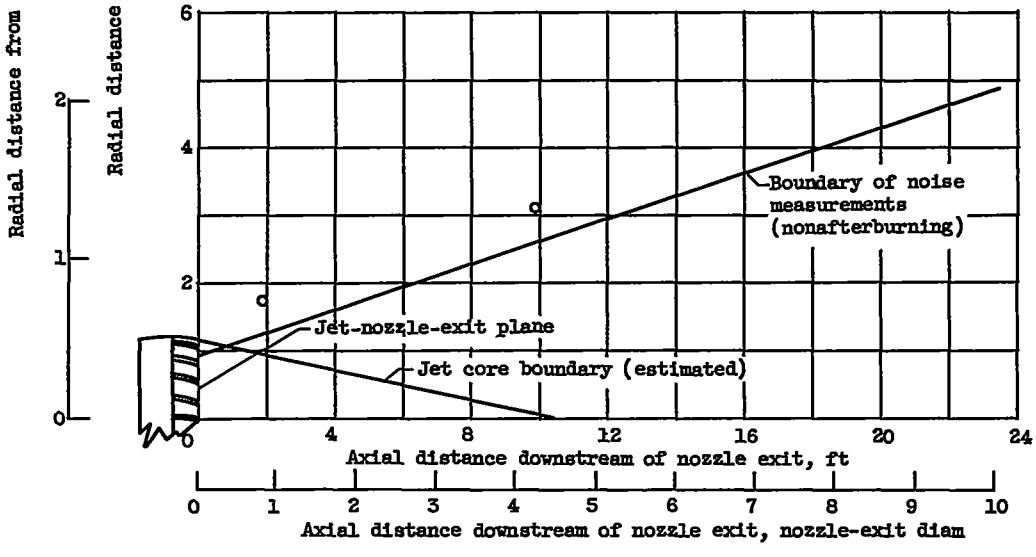

(c) Free field; afterburning.

Figure 5. - Concluded. Locus of near-field-noise measurements.

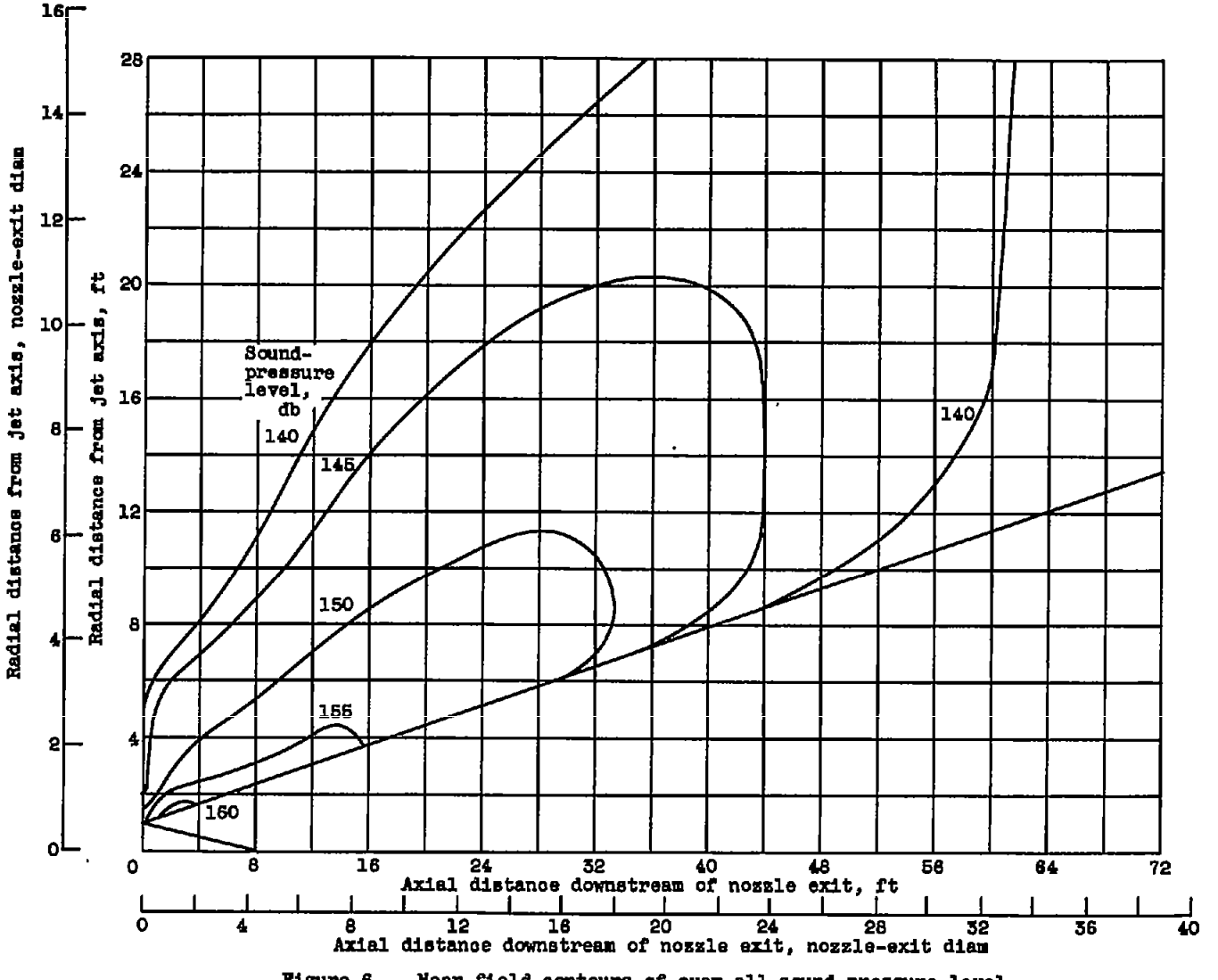

Figure 6. - Near-field contours of over-all sound-pressure level.

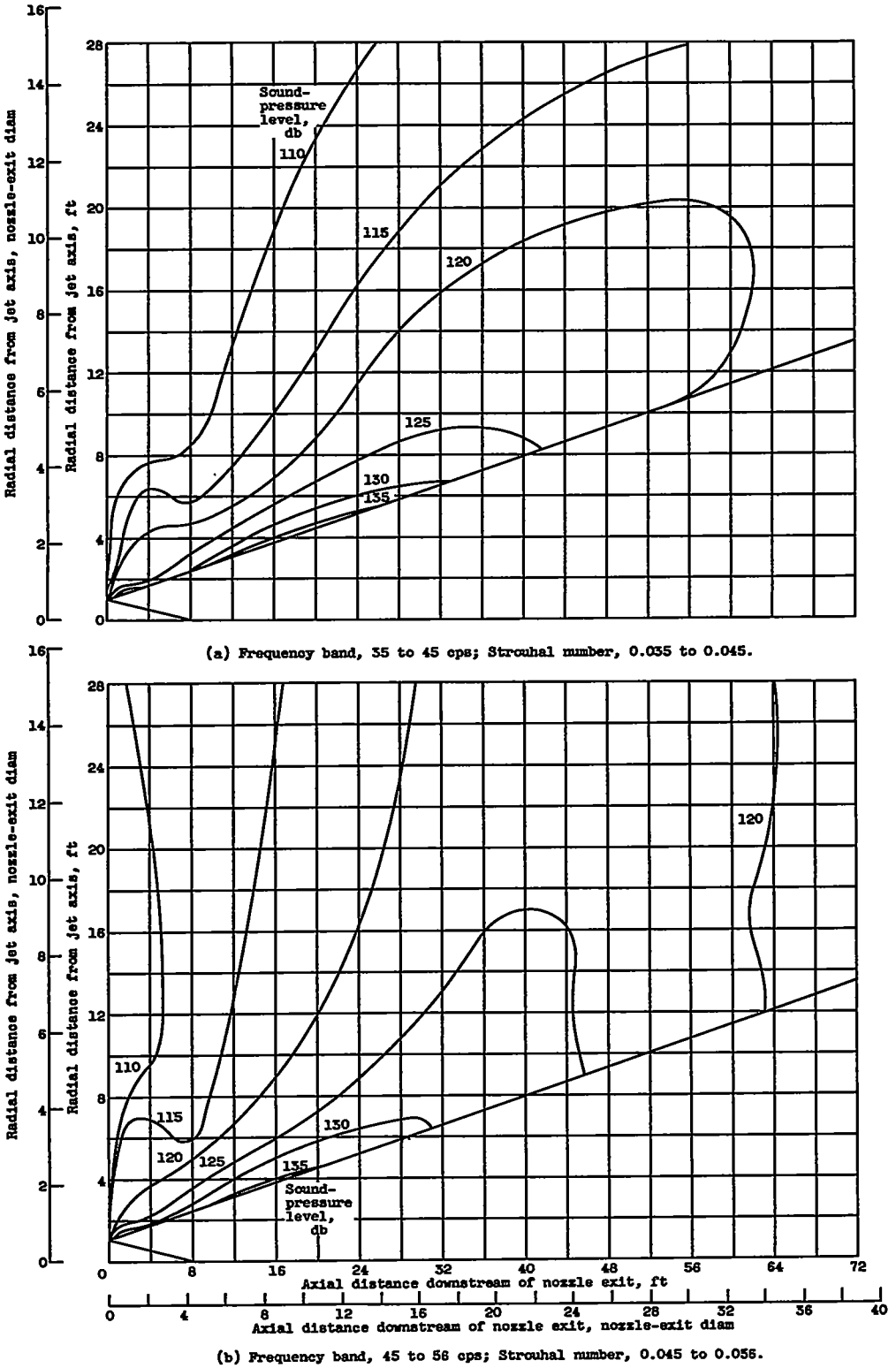

(a) Frequency band, 35 to 45 cps; Strouhal number, 0.035 to 0.045.

(b) Frequency band, 45 to 56 cps; Strouhal number, 0.045 to 0.056.

Figure 7. - Near-field contours of 1/3-octave-band sound-pressure levels.

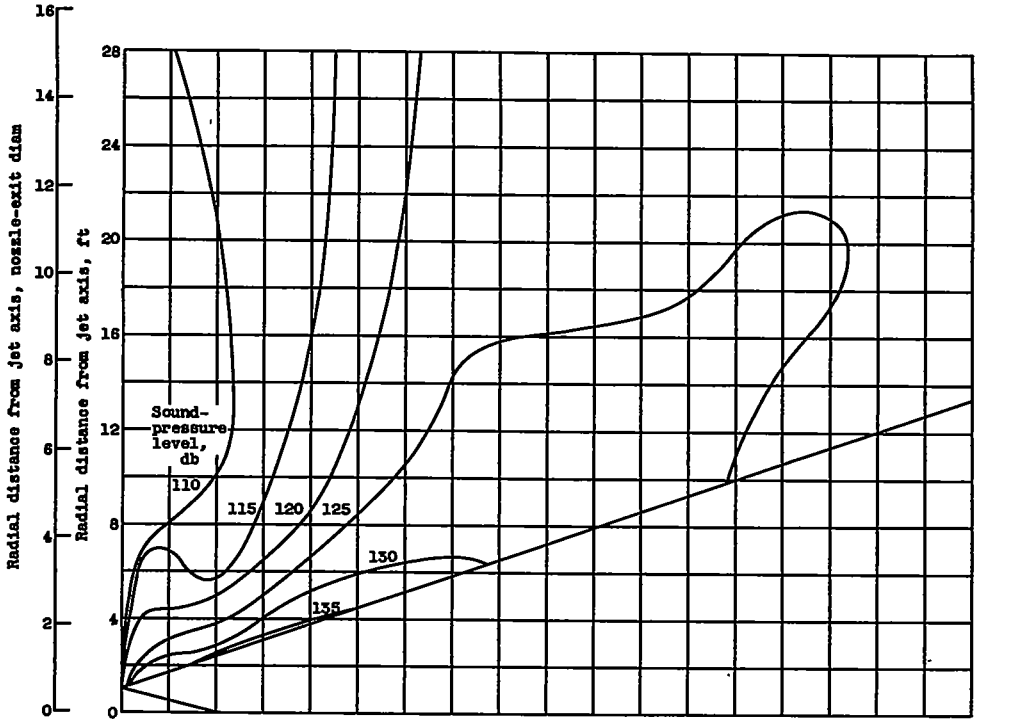

(c) Frequency band, 56 to 71 cps; Strouhal number, 0.056 to 0.071.

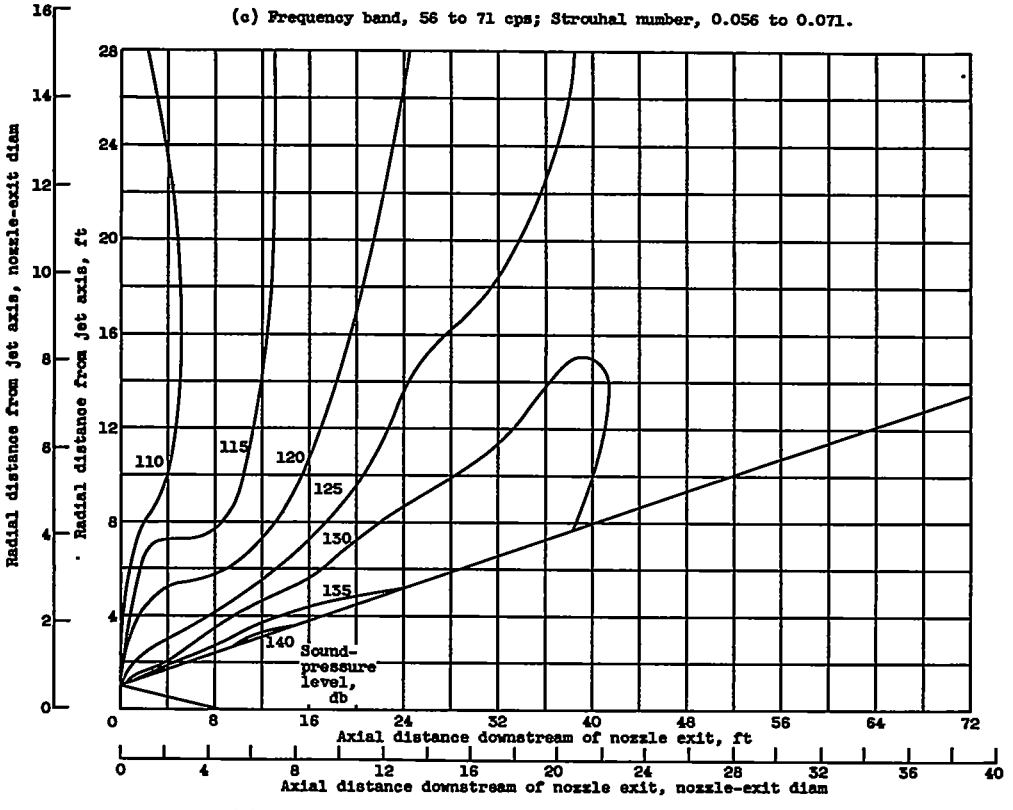

(d) Frequency band, 71 to 89 cps; Strouhal number, 0.071 to 0.089.

Figure 7. - Continued. Near-field contours of 1/3-octave-band sound-pressure levels.

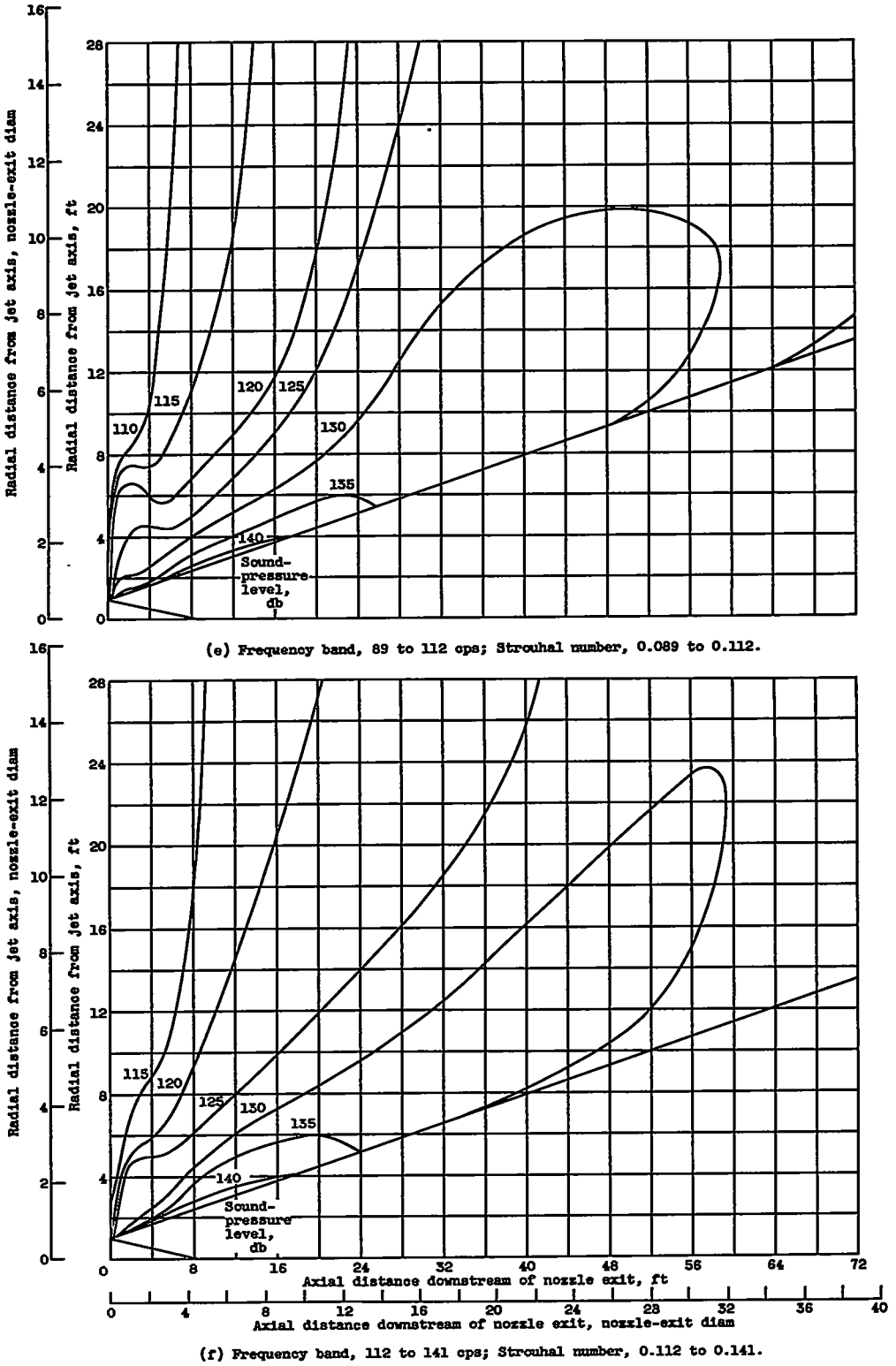

(e) Frequency band, 89 to 112 cps; Strouhal number, 0.089 to 0.112.

(f) Frequency band, 112 to 141 cps; Strouhal number, 0.112 to 0.141.

Figure 7. - Continued. Near-field contours of 1/3-octave-band sound-pressure levels.

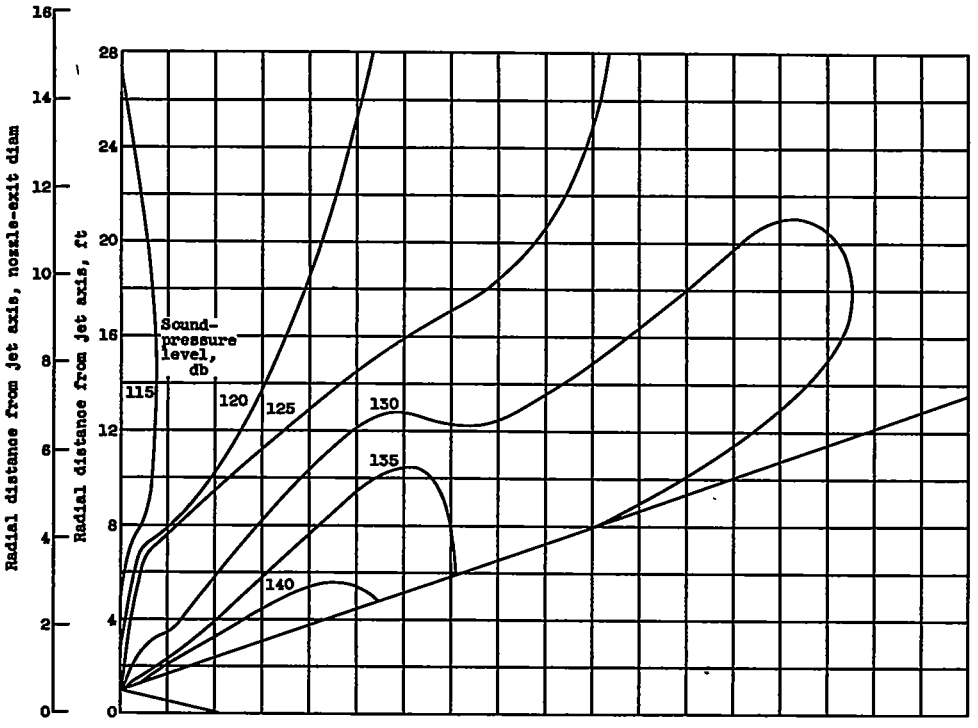

(g) Frequency band, 141 to 178 cps; Strouhal number, 0.141 to 0.178.

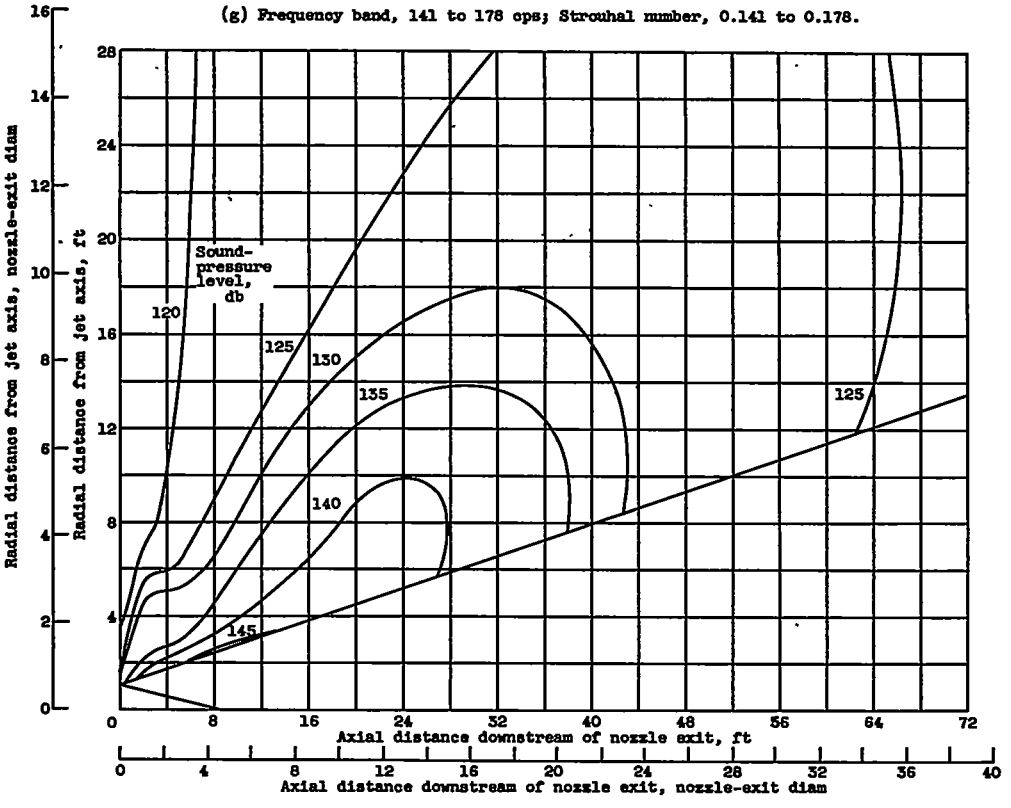

(h) Frequency band, 178 to 224 cps; Strouhal number, 0.178 to 0.224.

Figure 7. - Continued. Near-field contours of 1/3-octave-band sound-pressure levels.

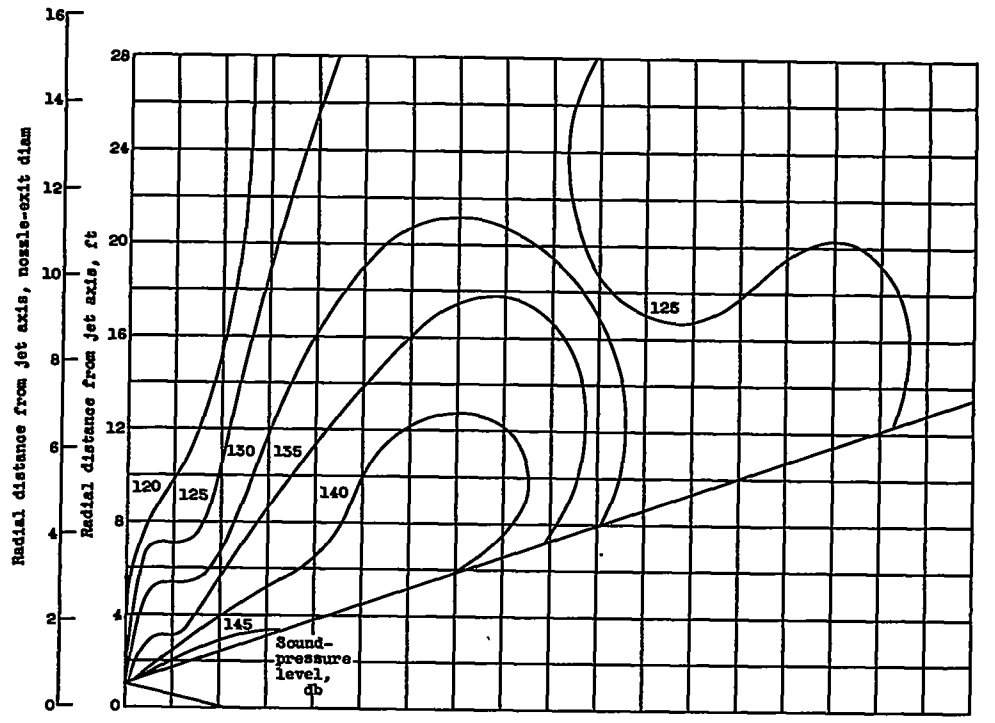

(i) Frequency band, 224 to 282 cps; Strouhal number, 0.224 to 0.282.

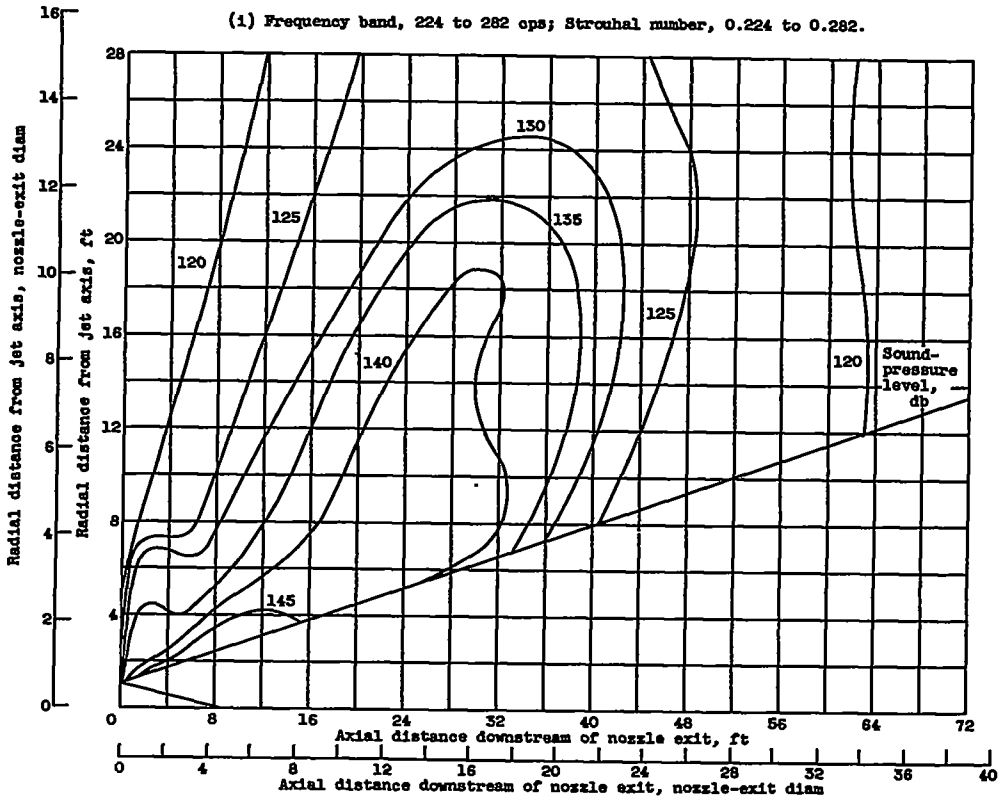

(j) Frequency band, 282 to 355 cps; Strouhal number, 0.282 to 0.355.

Figure 7. - Continued. Near-field contours of 1/3-octave-band sound-pressure levels.

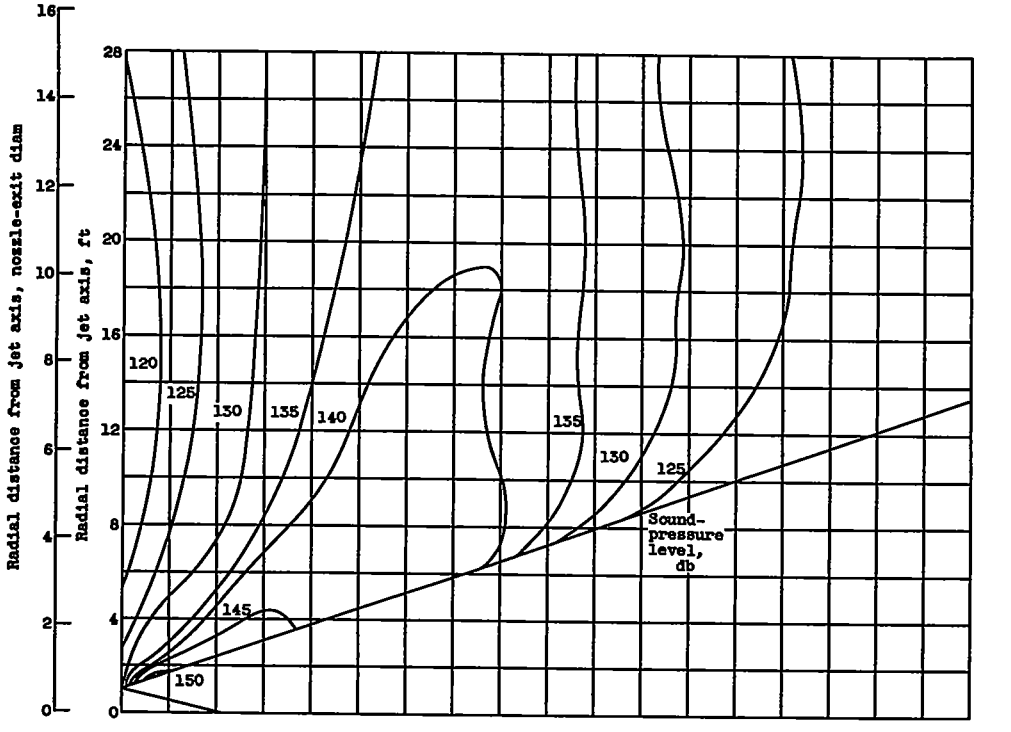

(k) Frequency band, 355 to 447 cps; Strouhal number, 0.355 to 0.447.

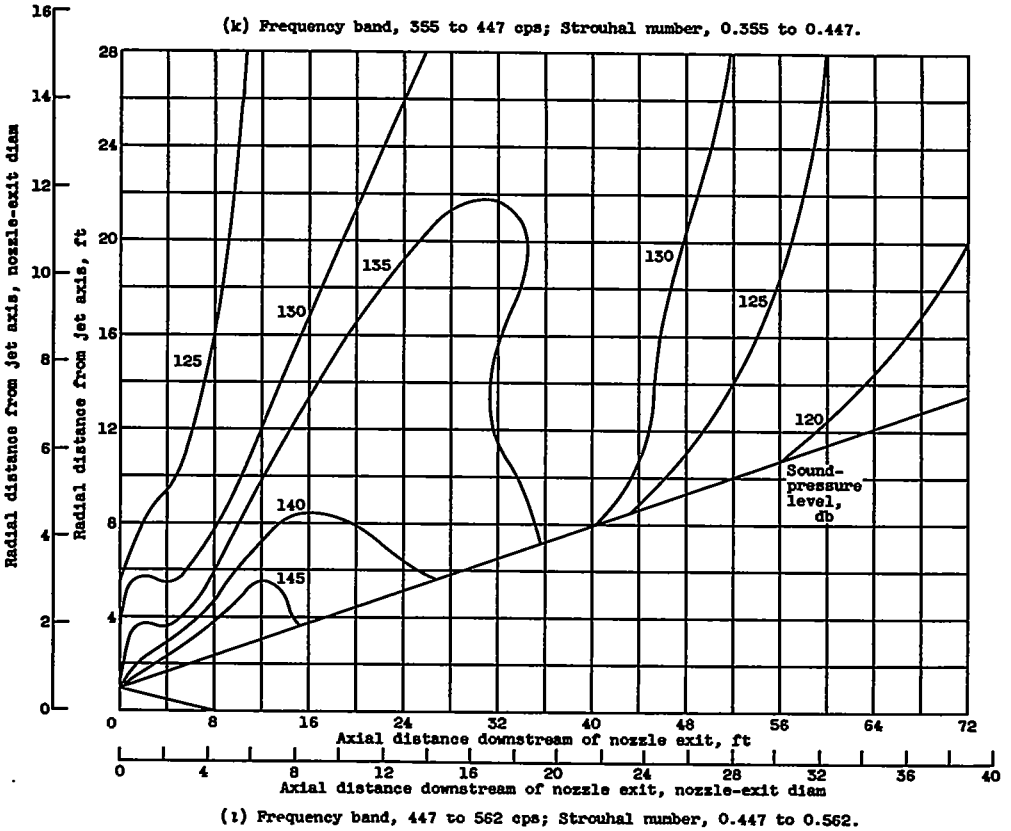

(l) Frequency band, 447 to 562 cps; Strouhal number, 0.447 to 0.562.

Figure 7. - Continued. Near-field contours of 1/3-octave-band sound-pressure levels.

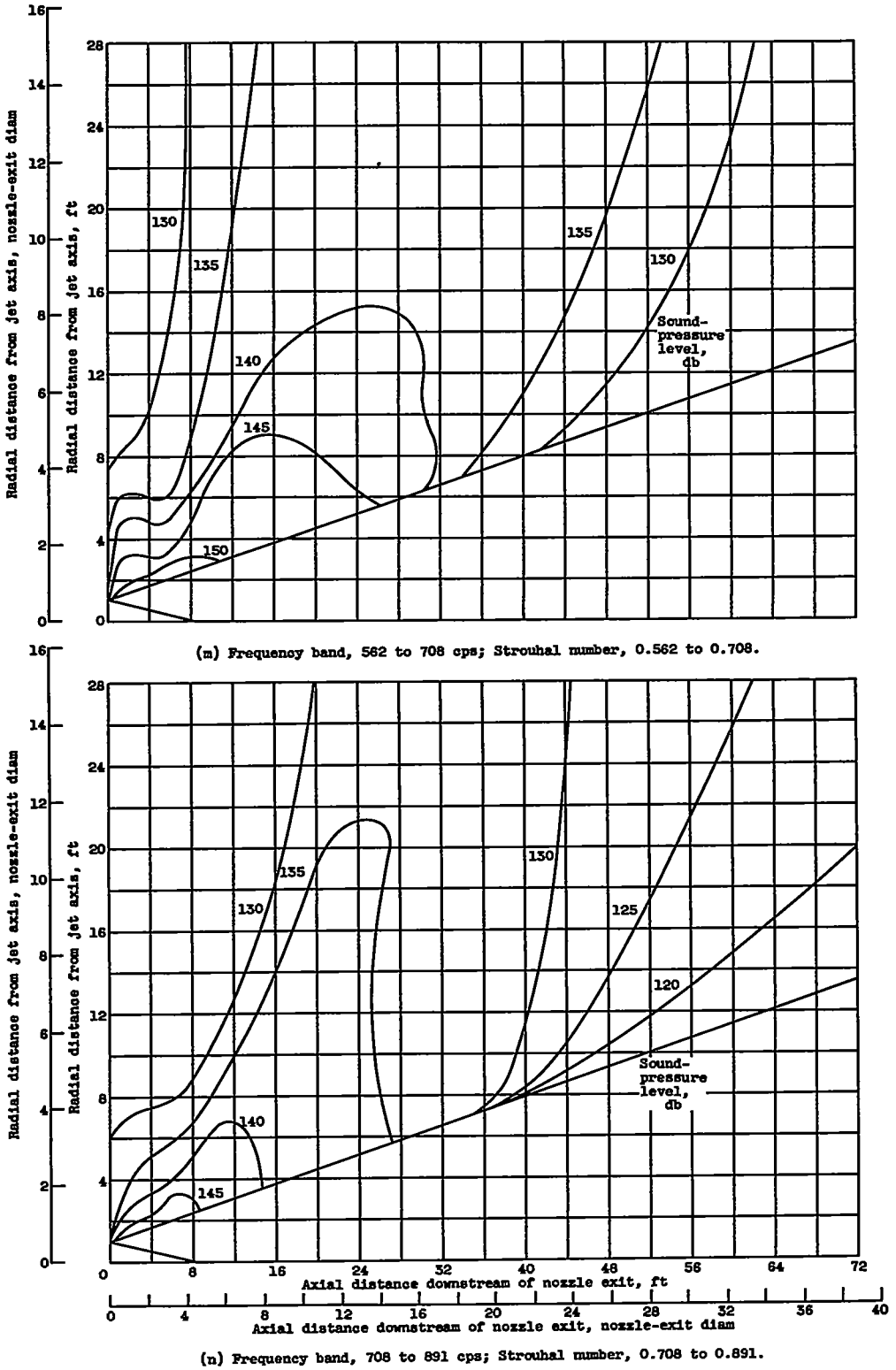

Figure 7. - Continued. Near-field contours of 1/3-octave-band sound-pressure levels.

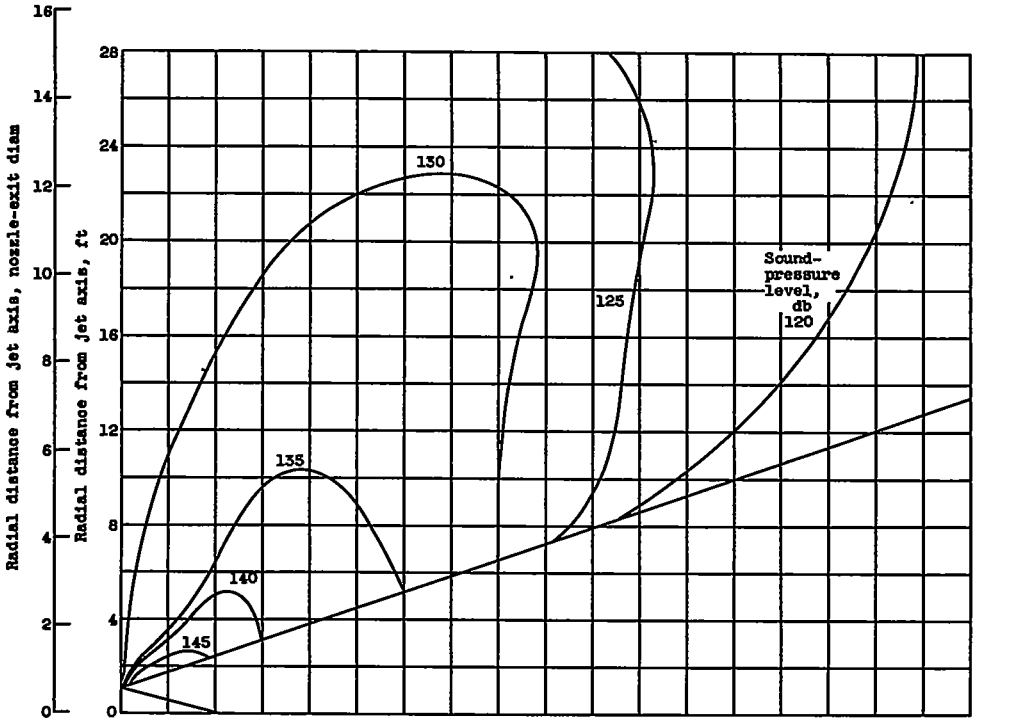

(o) Frequency band, 891 to 1120 cps; Strouhal number, 0.891 to 1.120.

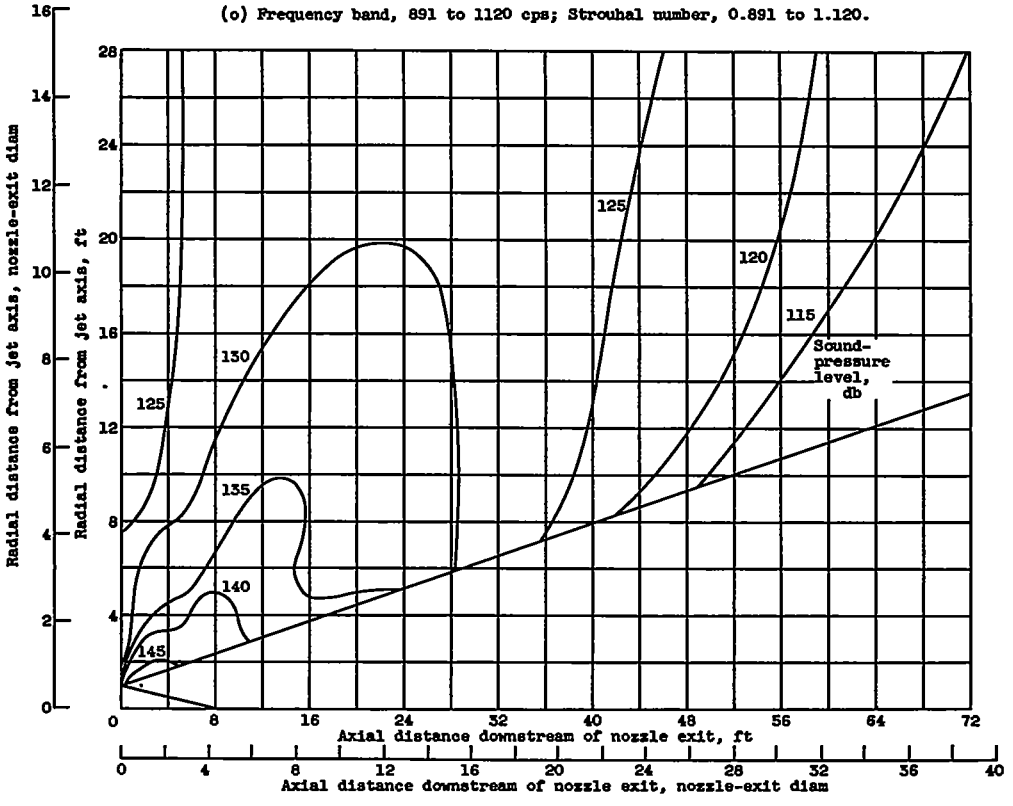

(p) Frequency band, 1120 to 1410 cps; Strouhal number, 1.120 to 1.410.

Figure 7. - Continued. Near-field contours of 1/3-octave-band sound-pressure levels.

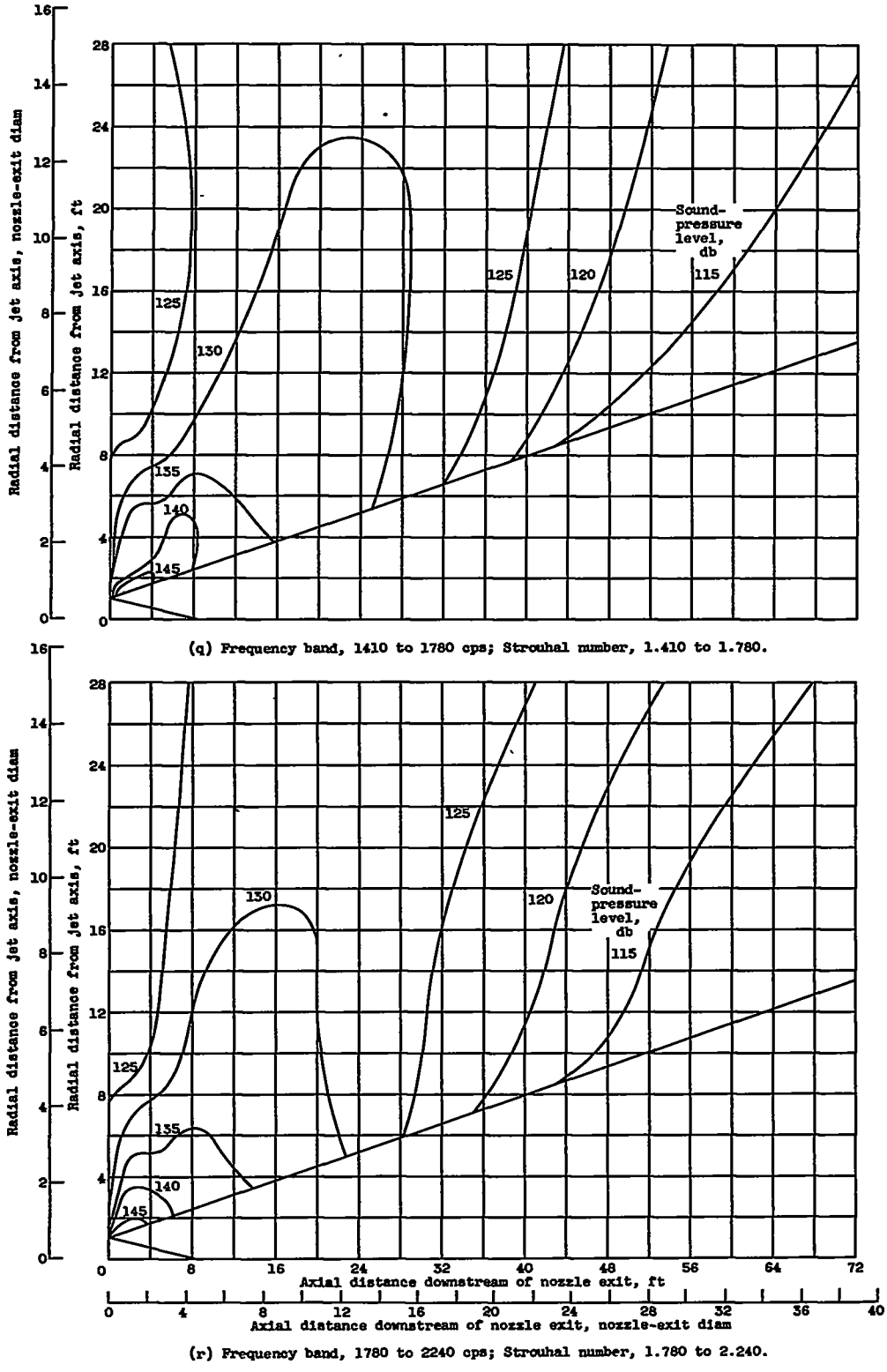

(q) Frequency band, 1410 to 1780 cps; Strouhal number, 1.410 to 1.780.

(r) Frequency band, 1780 to 2240 cps; Strouhal number, 1.780 to 2.240.

Figure 7. - Continued. Near-field contours of 1/3-octave-band sound-pressure levels.

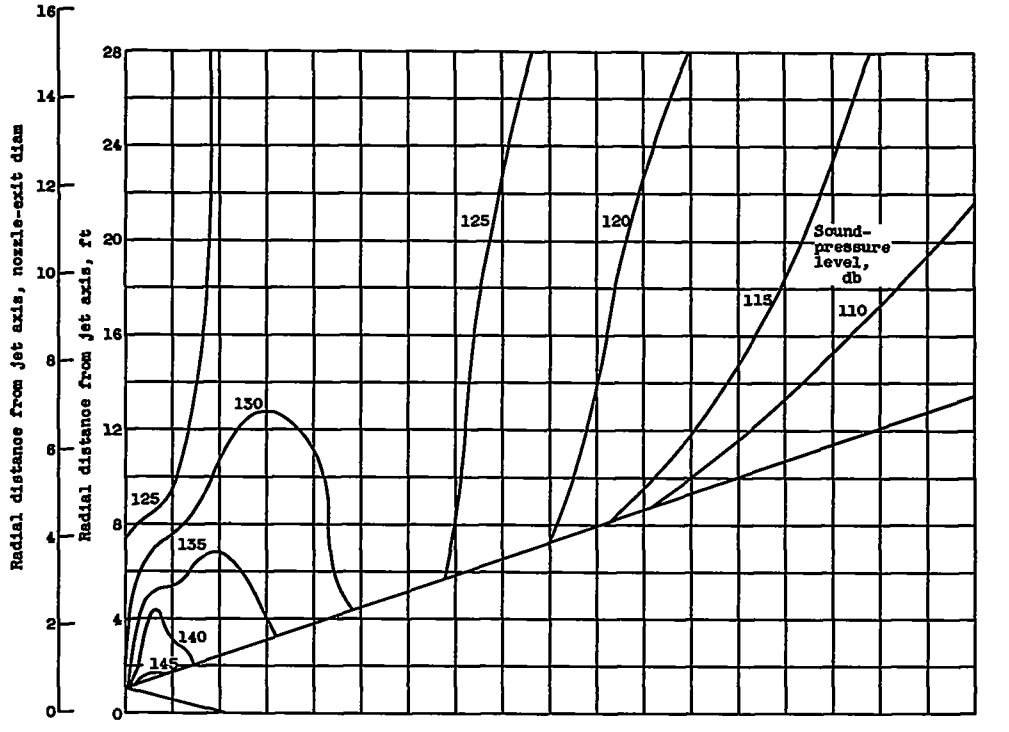

(s) Frequency band, 2240 to 2820 cps; Strouhal number, 2.240 to 2.820

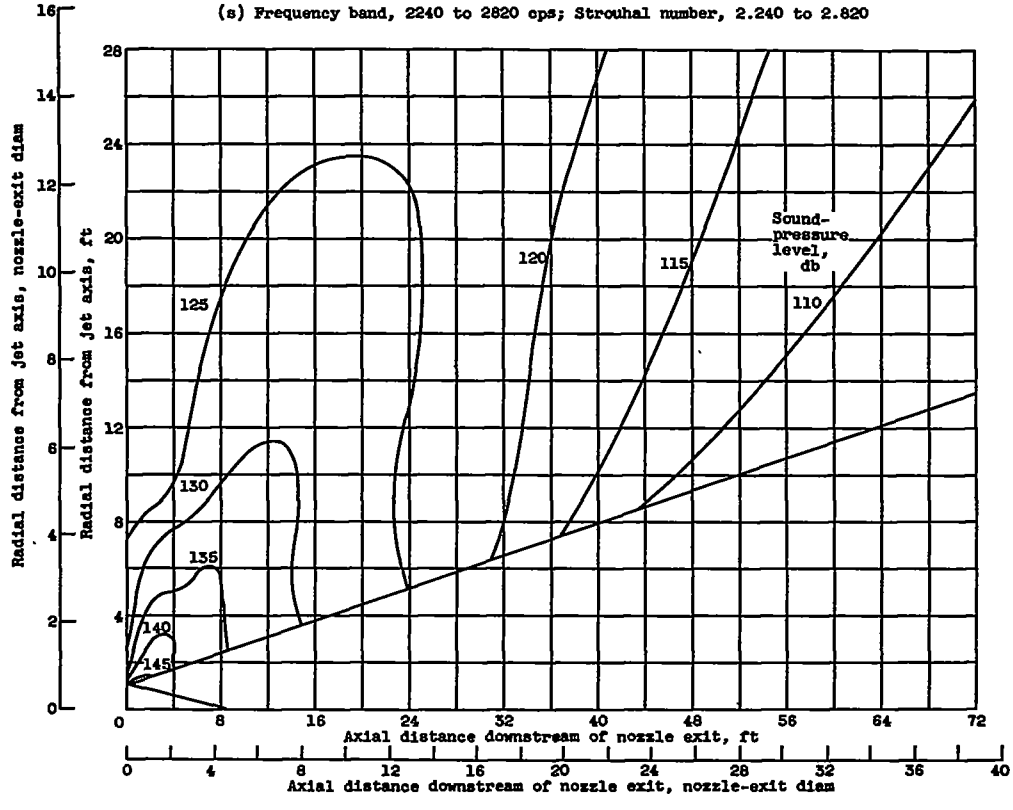

(t) Frequency band, 2820 to 3550 cps; Strouhal number, 2.820 to 3.550.

Figure 7. - Continued. Near-field contours of 1/3-octave-band sound-pressure levels.

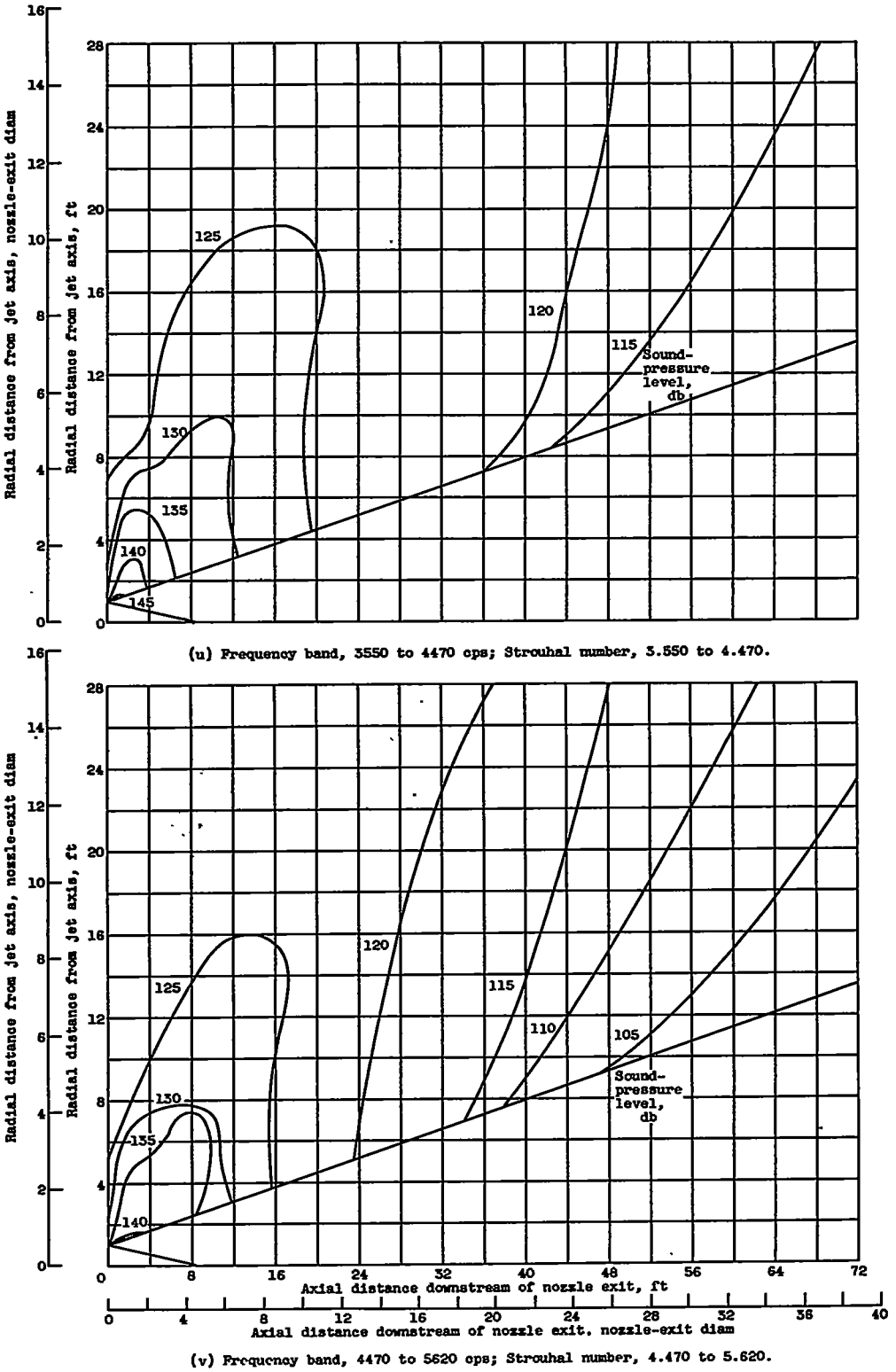

Figure 7. - Continued. Near-field contours of 1/3-octave-band sound-pressure levels.

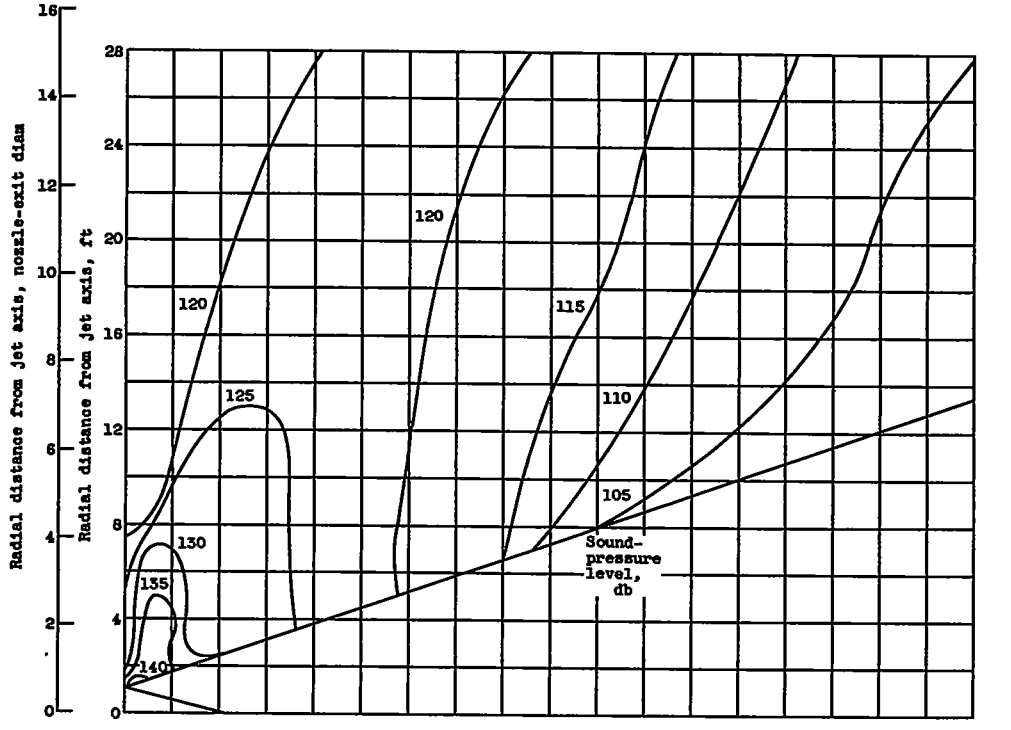

(w) Frequency band, 5620 to 7080 cps; Strouhal number, 5.620 to 7.080.

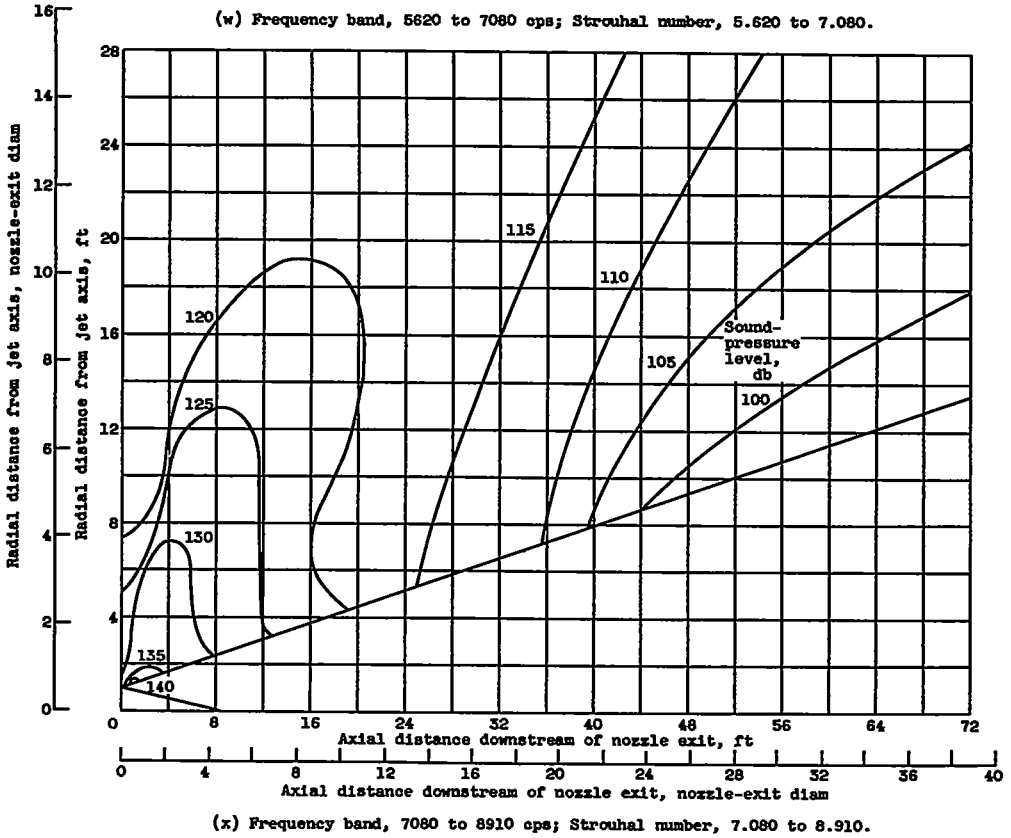

(x) Frequency band, 7080 to 8910 cps; Strouhal number, 7.080 to 8.910.

Figure 7. - Continued. Near-field contours of 1/3-octave-band sound-pressure levels.

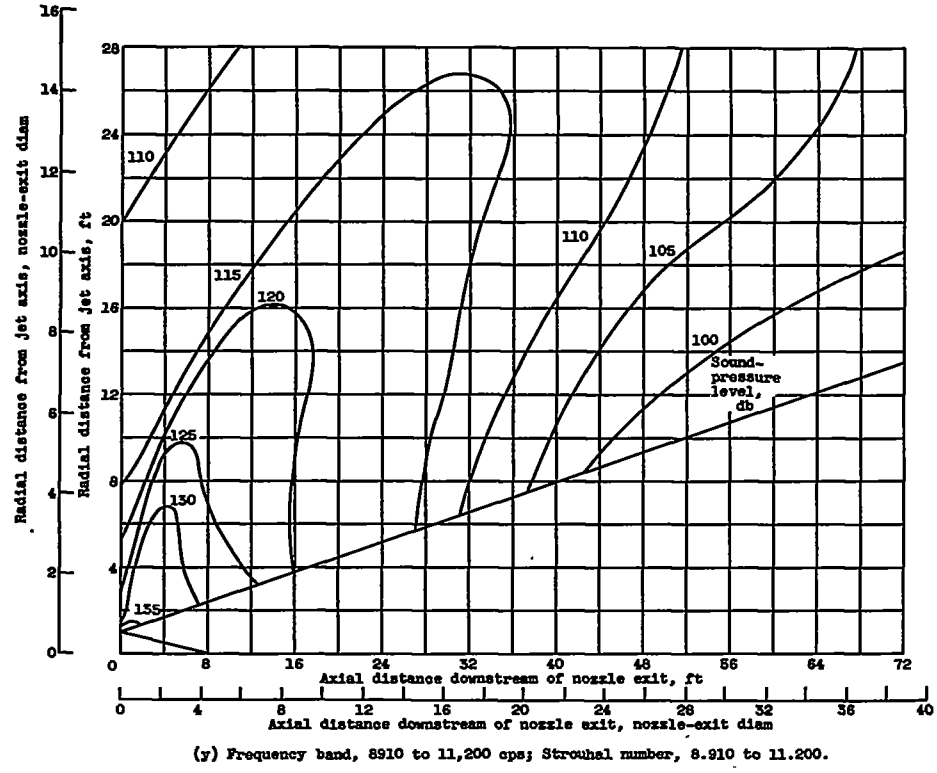

(y) Frequency band, 8910 to 11,200 cps; Strouhal number, 8.910 to 11.200.

Figure 7. - Concluded. Near-field contours of 1/3-octave-band sound-pressure levels.

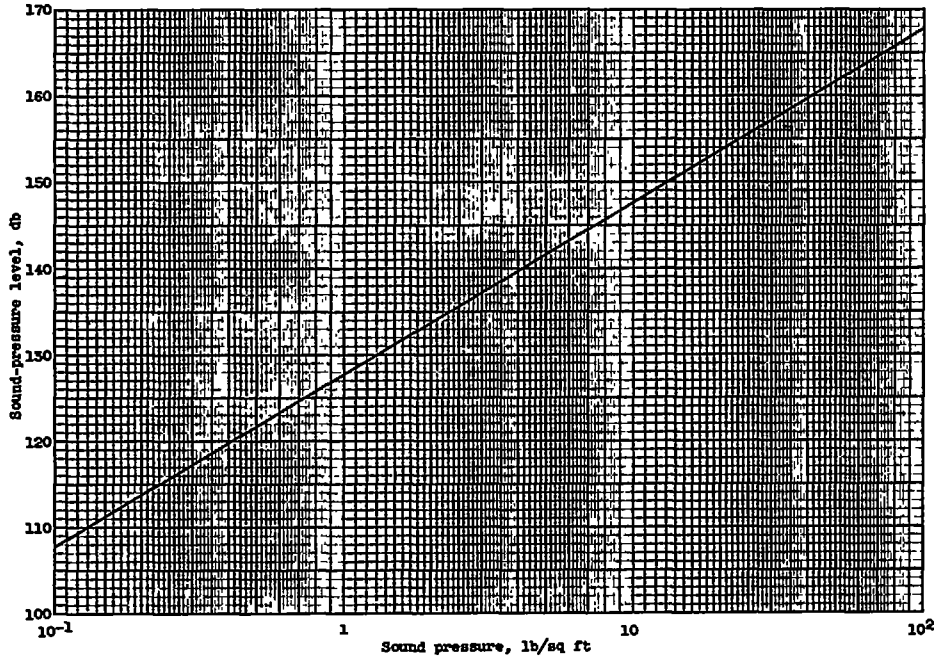

Figure 8. - Sound-pressure level as function of sound pressure. Sound-pressure level (db) = 20 log $\left(\frac{p}{p_o}\right)$. (Reference pressure p_o, 2×10^{-4} dyne/cm^2; p, acoustical pressure.)

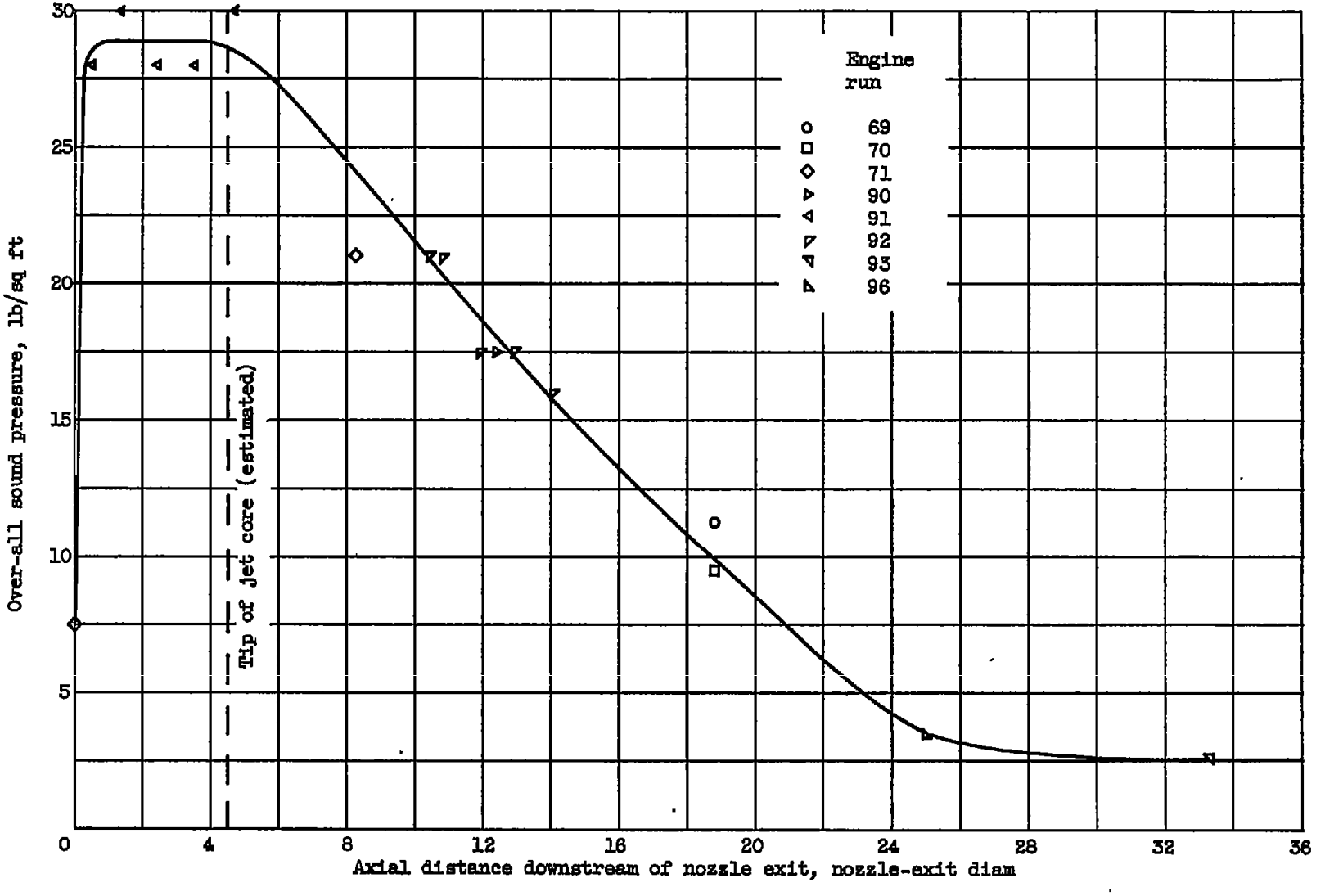

Figure 9. - Over-all sound pressure along jet boundary.

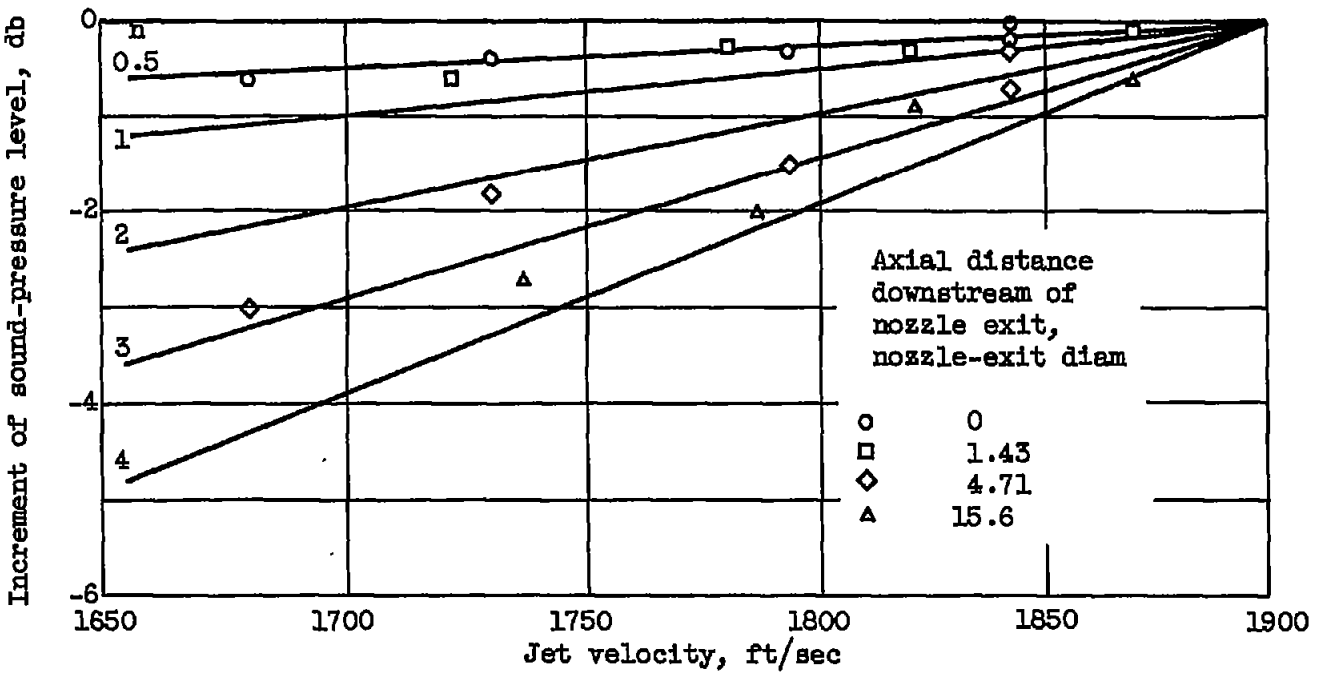

Figure 10. - Effect of jet velocity on over-all sound-pressure level along jet boundary.

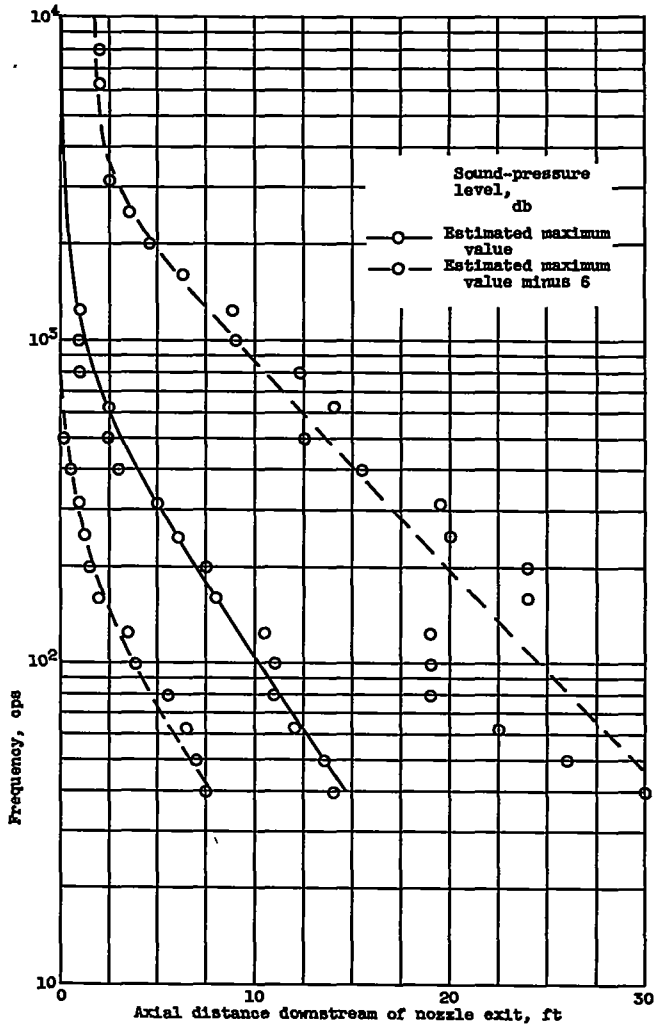

(a) Semilogarithmic plot.

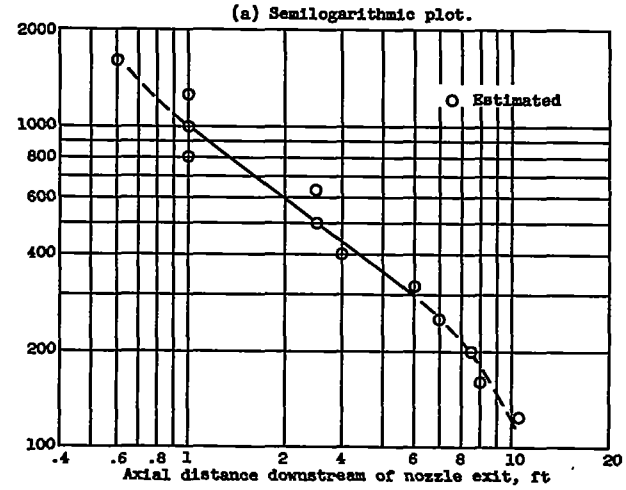

(b) Logarithmic plot corresponding to maximum sound-pressure level.

Figure 11. - Frequency of acoustical sources as function of distance downstream of jet-nozzle exit.

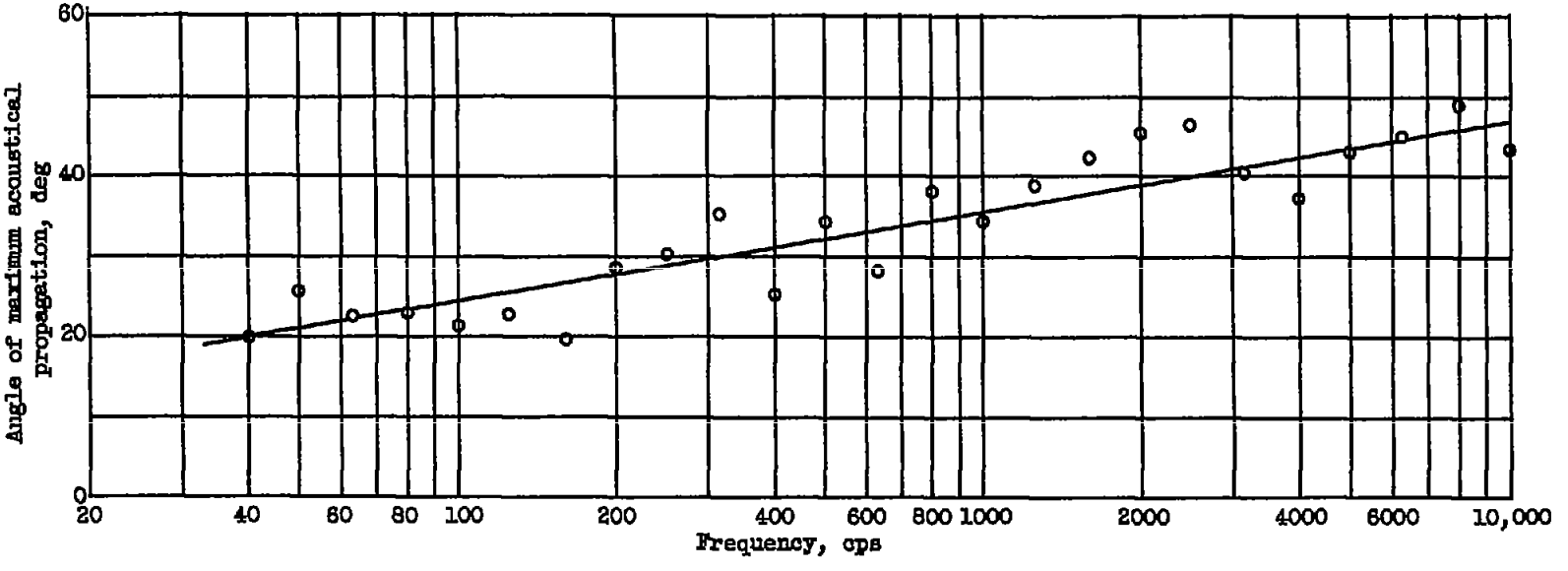

Figure 12. - Effect of frequency on angle of maximum acoustical propagation.

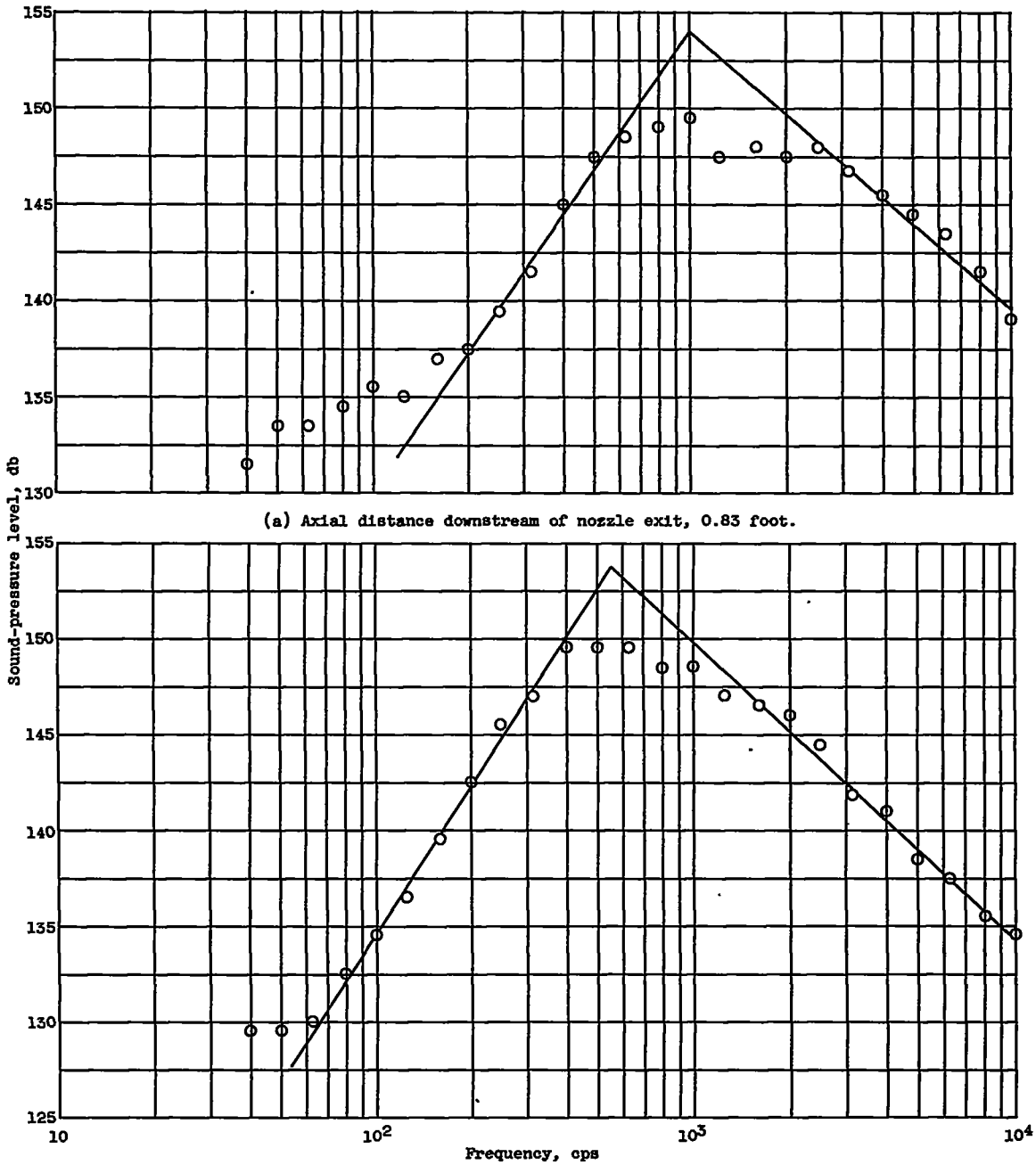

(a) Axial distance downstream of nozzle exit, 0.83 foot.

(b) Axial distance downstream of nozzle exit, 2.42 feet.

Figure 13. - Noise spectra along jet boundary.

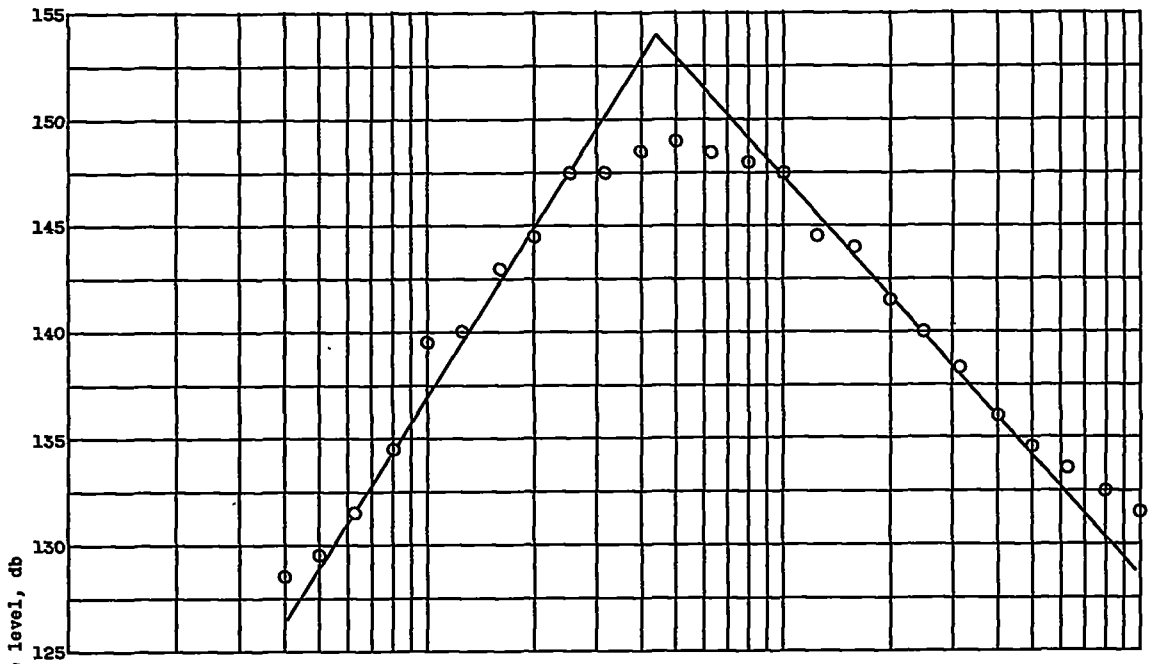

(c) Axial distance downstream of nozzle exit, 4.50 feet.

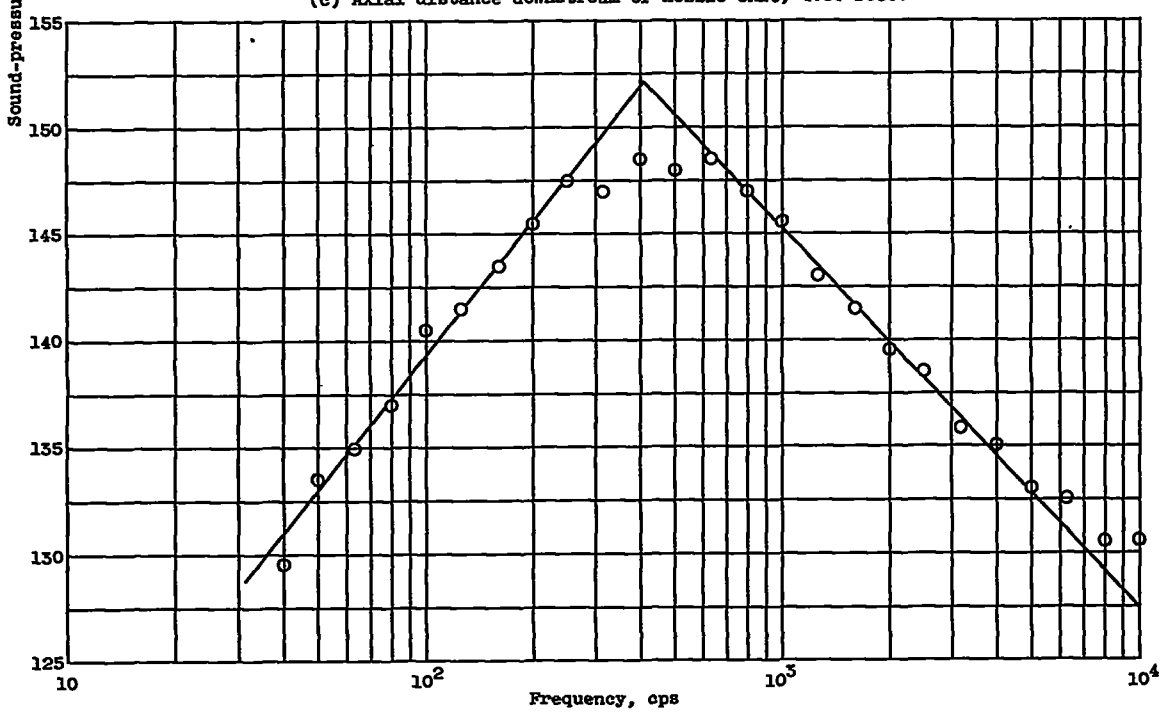

(d) Axial distance downstream of nozzle exit, 6.58 feet.

Figure 13. - Continued. Noise spectra along jet boundary.

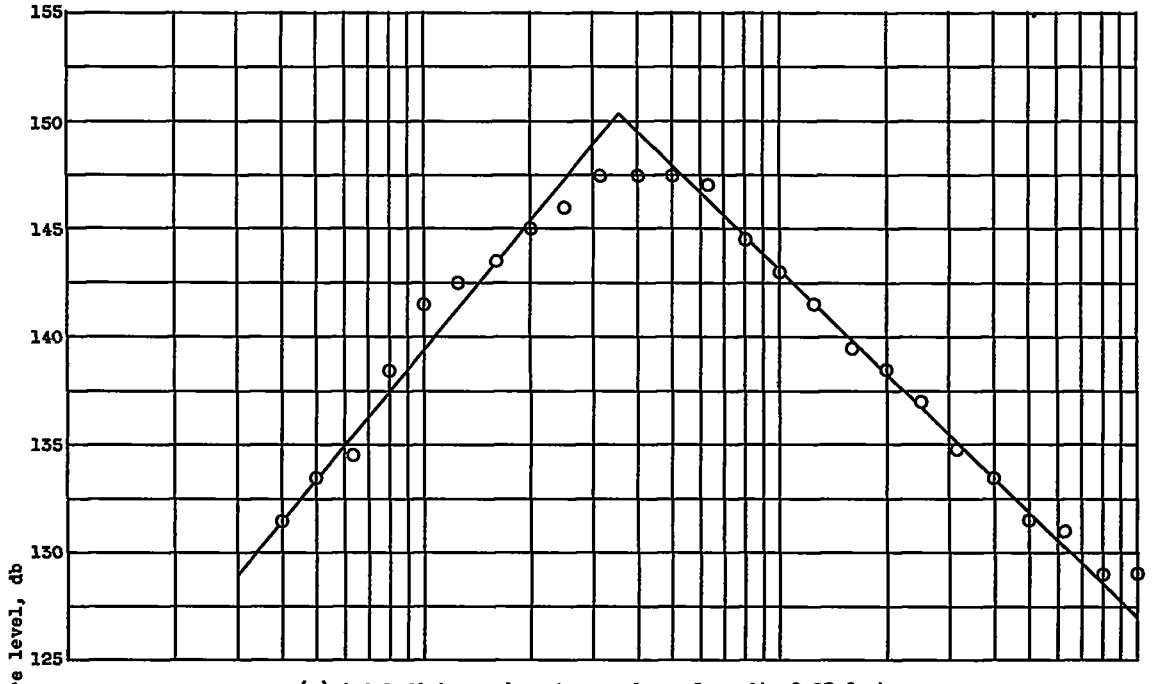

(e) Axial distance downstream of nozzle exit, 8.67 feet.

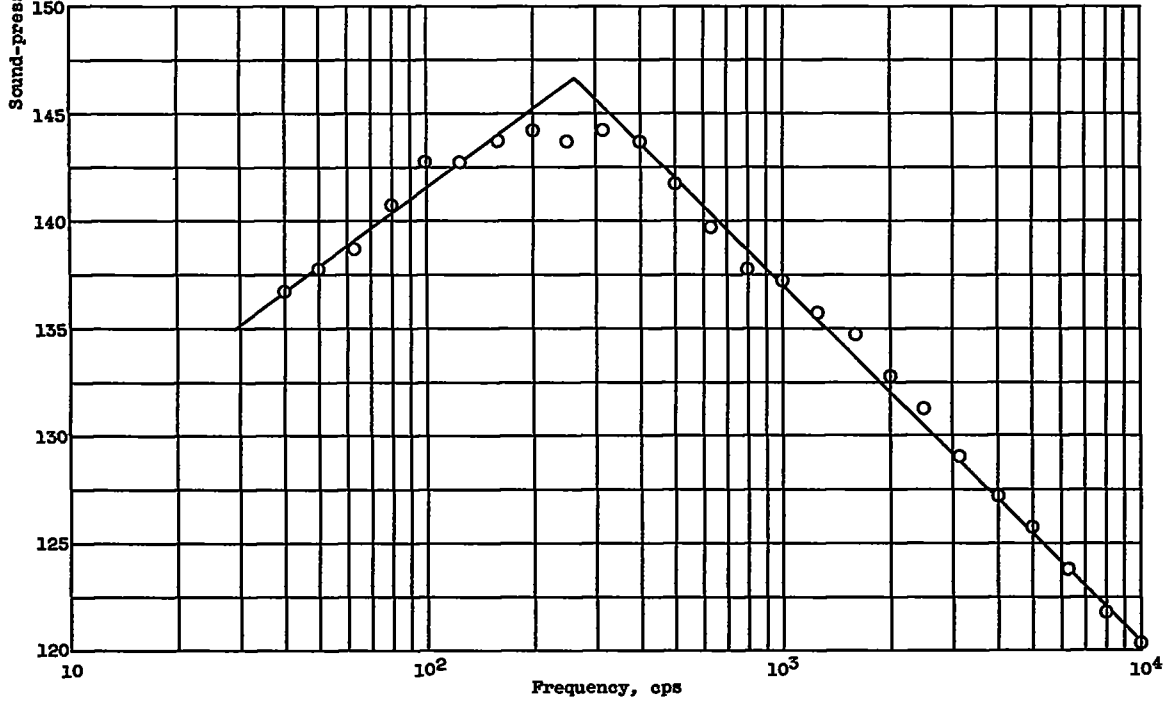

(f) Axial distance downstream of nozzle exit, 15.45 feet.

Figure 13. - Continued. Noise spectra along jet boundary.

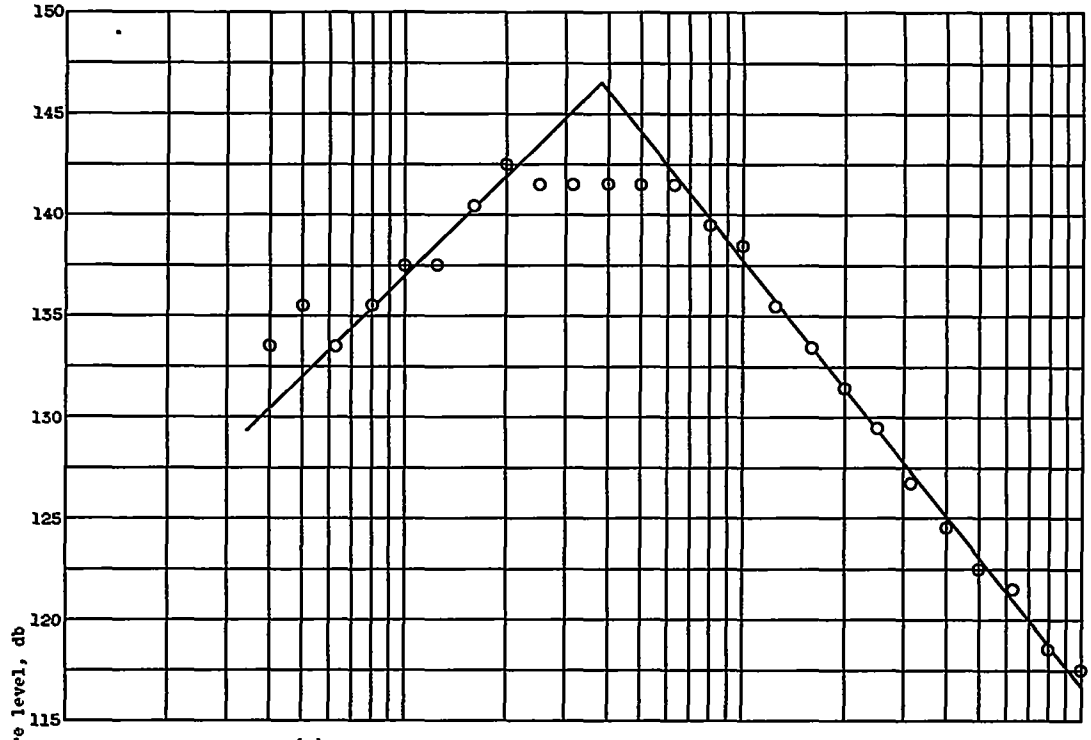

(g) Axial distance downstream of nozzle exit, 20 feet.

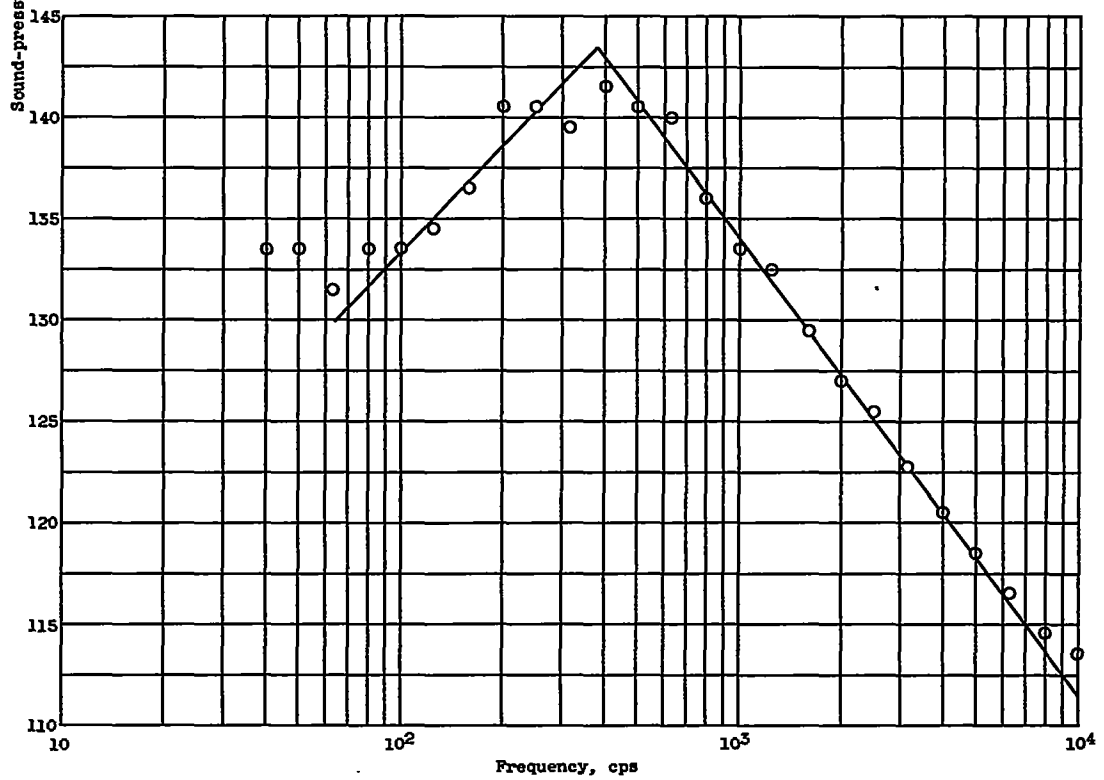

(h) Axial distance downstream of nozzle exit, 26 feet.

Figure 13. - Continued. Noise spectra along jet boundary.

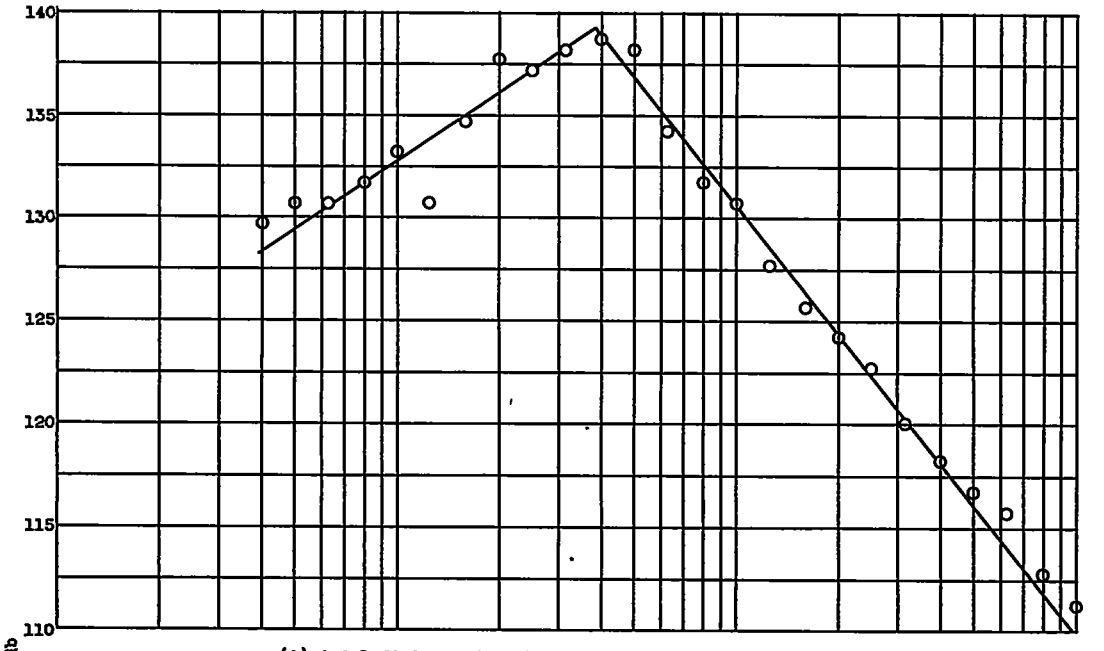

(i) Axial distance downstream of nozzle exit, 30.9 feet.

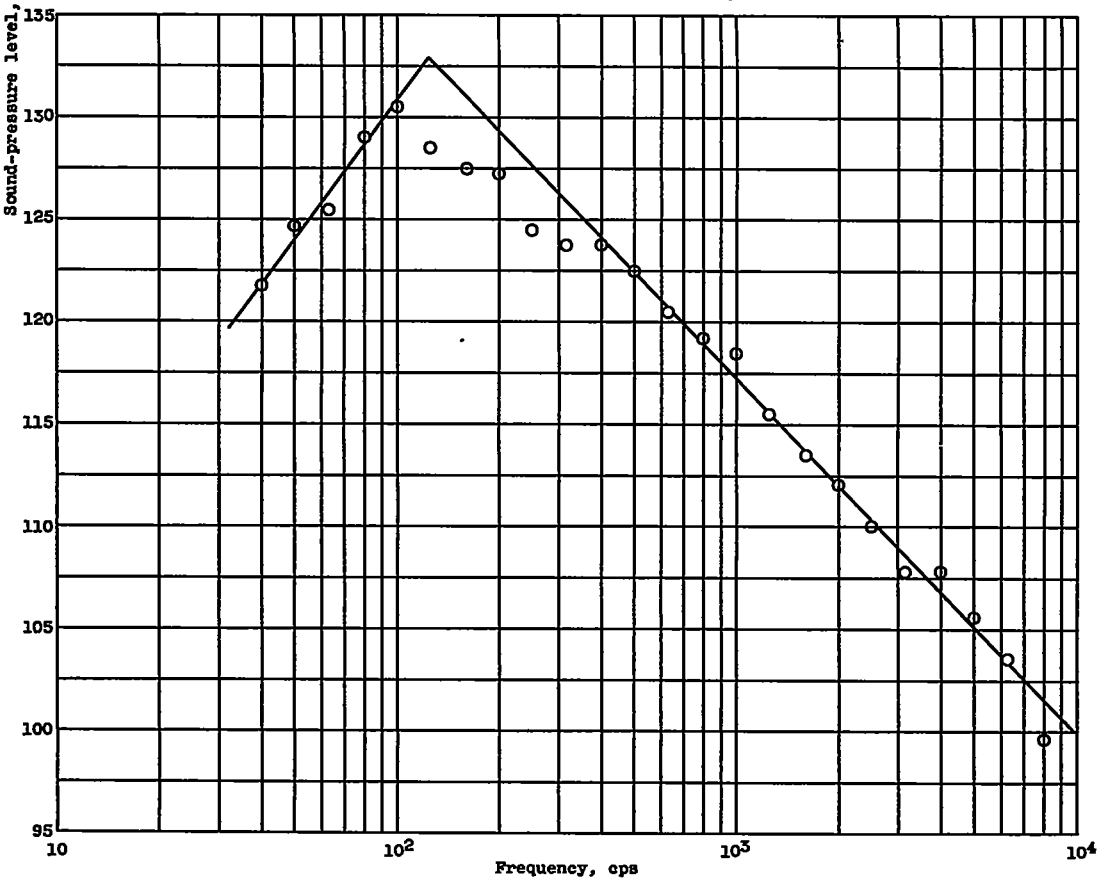

(j) Axial distance downstream of nozzle exit, 46.35 feet.

Figure 13. - Continued. Noise spectra along jet boundary.

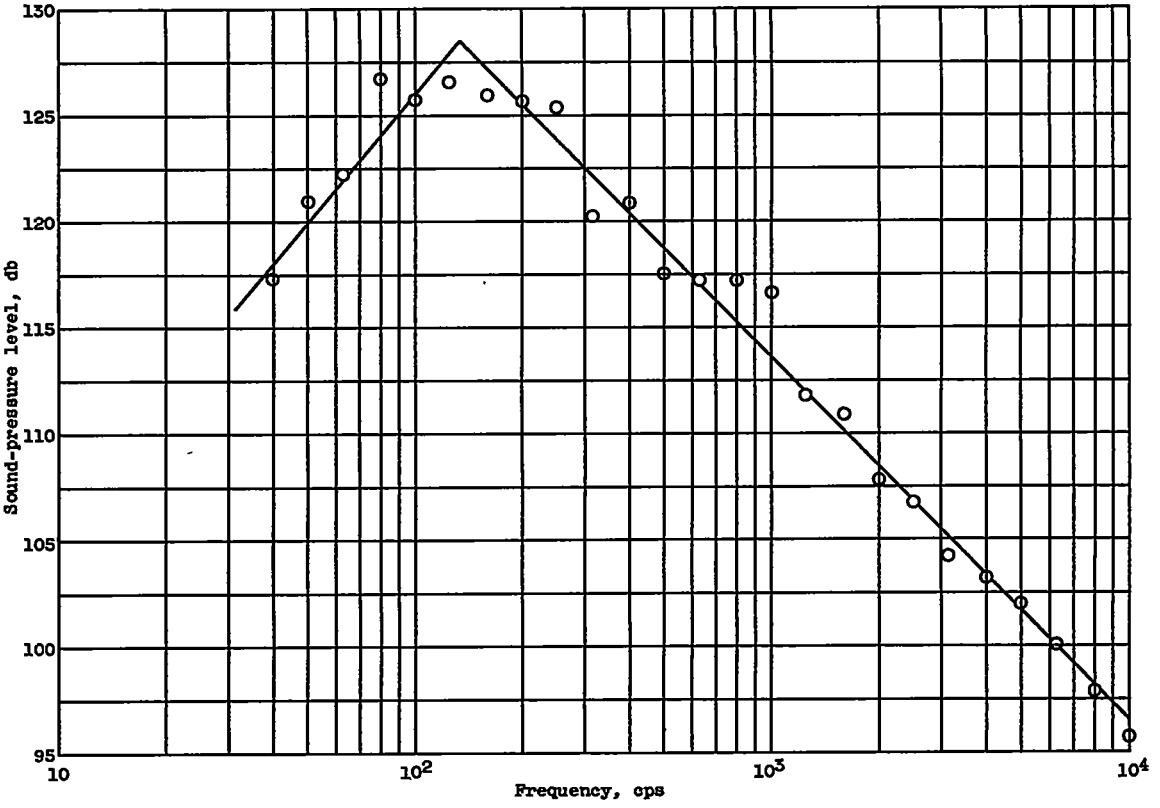

(k) Axial distance downstream of nozzle exit, 61.8 feet.

Figure 13. - Concluded. Noise spectra along jet boundary.

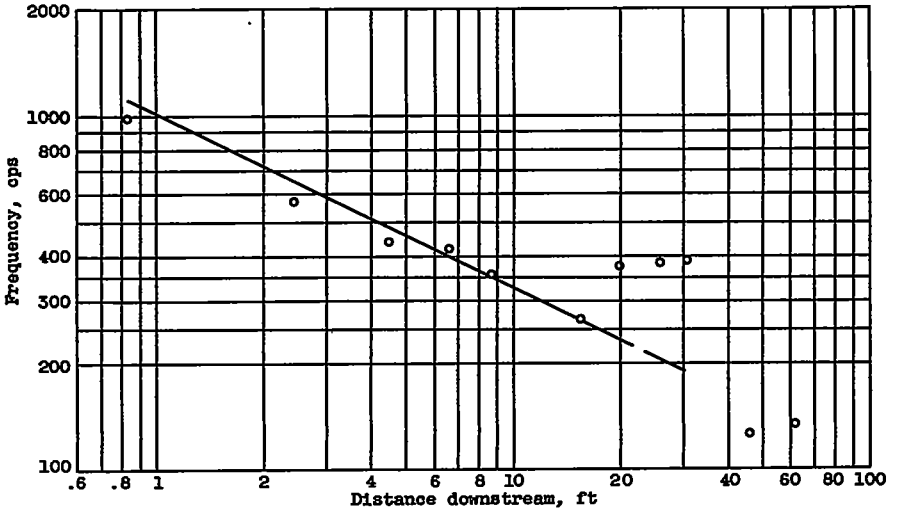

Figure 14. - Frequency of acoustical spectrum maximum as function of distance downstream of jet-nozzle exit.

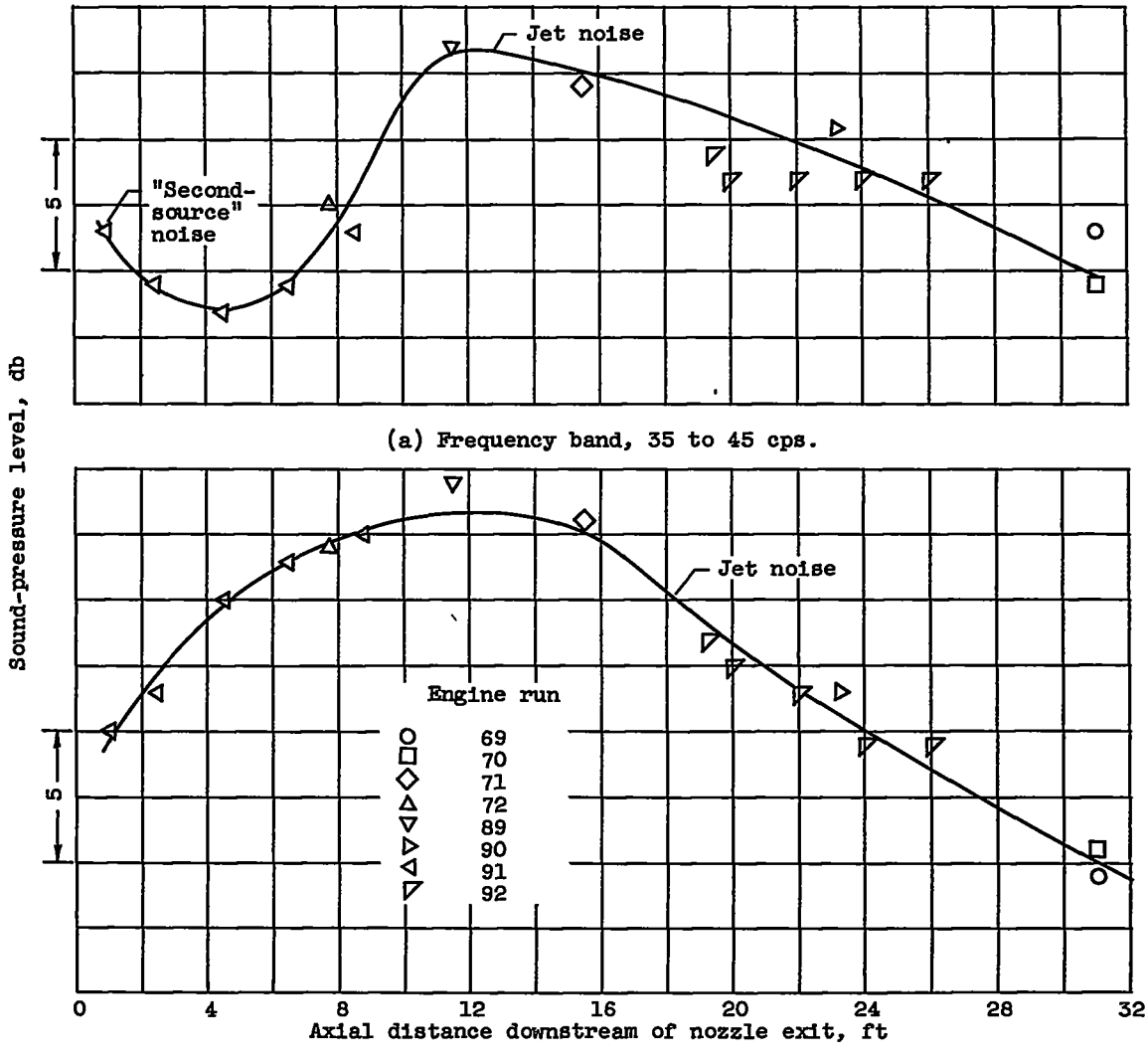

(a) Frequency band, 35 to 45 cps.

(b) Frequency band, 112 to 141 cps.

Figure 15. - Sound-pressure level along jet boundary.

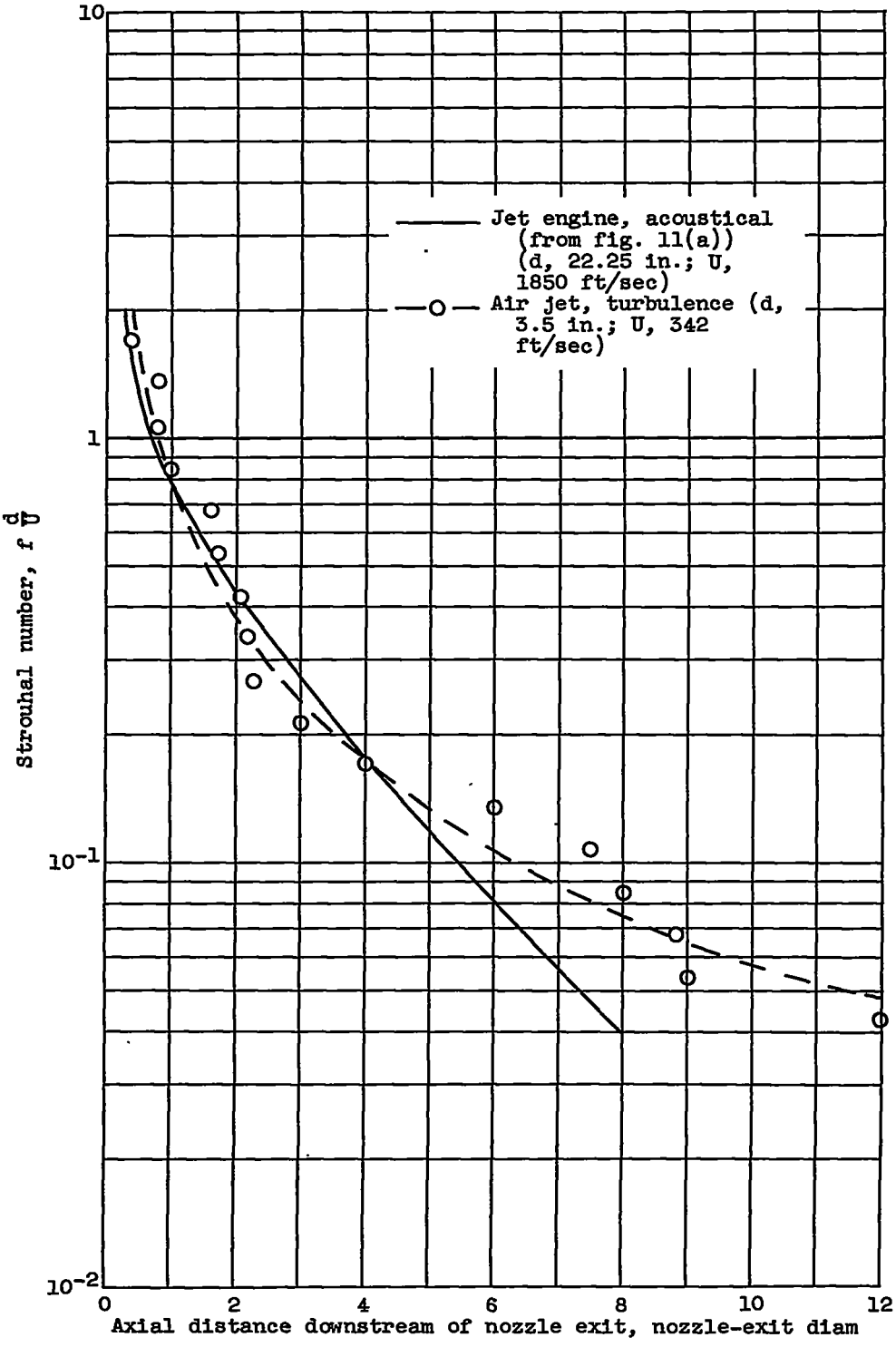

Figure 16. - Comparison of dimensionless distance downstream from jet-nozzle exit of jet-engine-noise and air-jet-turbulence maximums for given Strouhal numbers. (U, jet velocity; f, frequency; d, nozzle-exit diameter.)

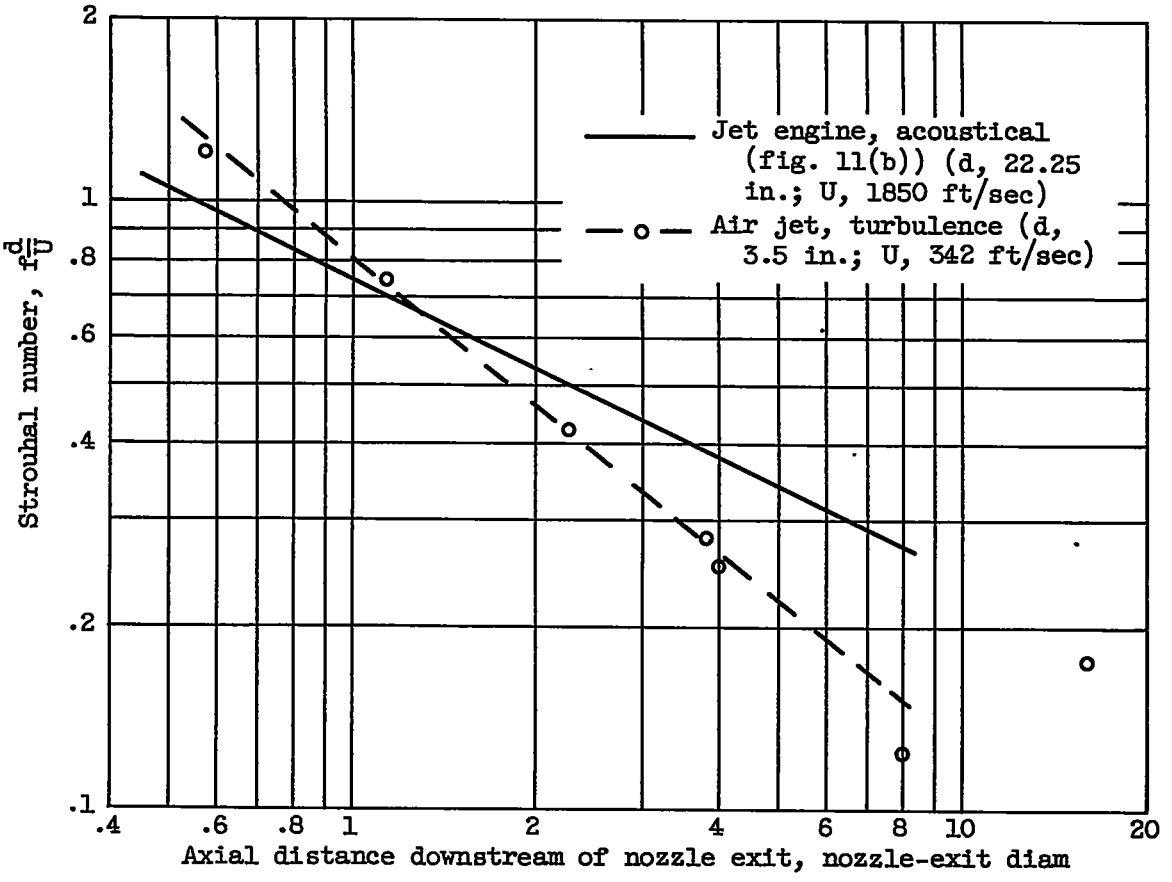

Figure 17. - Comparison of Strouhal numbers of acoustical and turbulence spectra maximums as function of dimensionless distance downstream of jet-nozzle exit. (U, jet velocity; f, frequency; d, nozzle-exit diameter.)

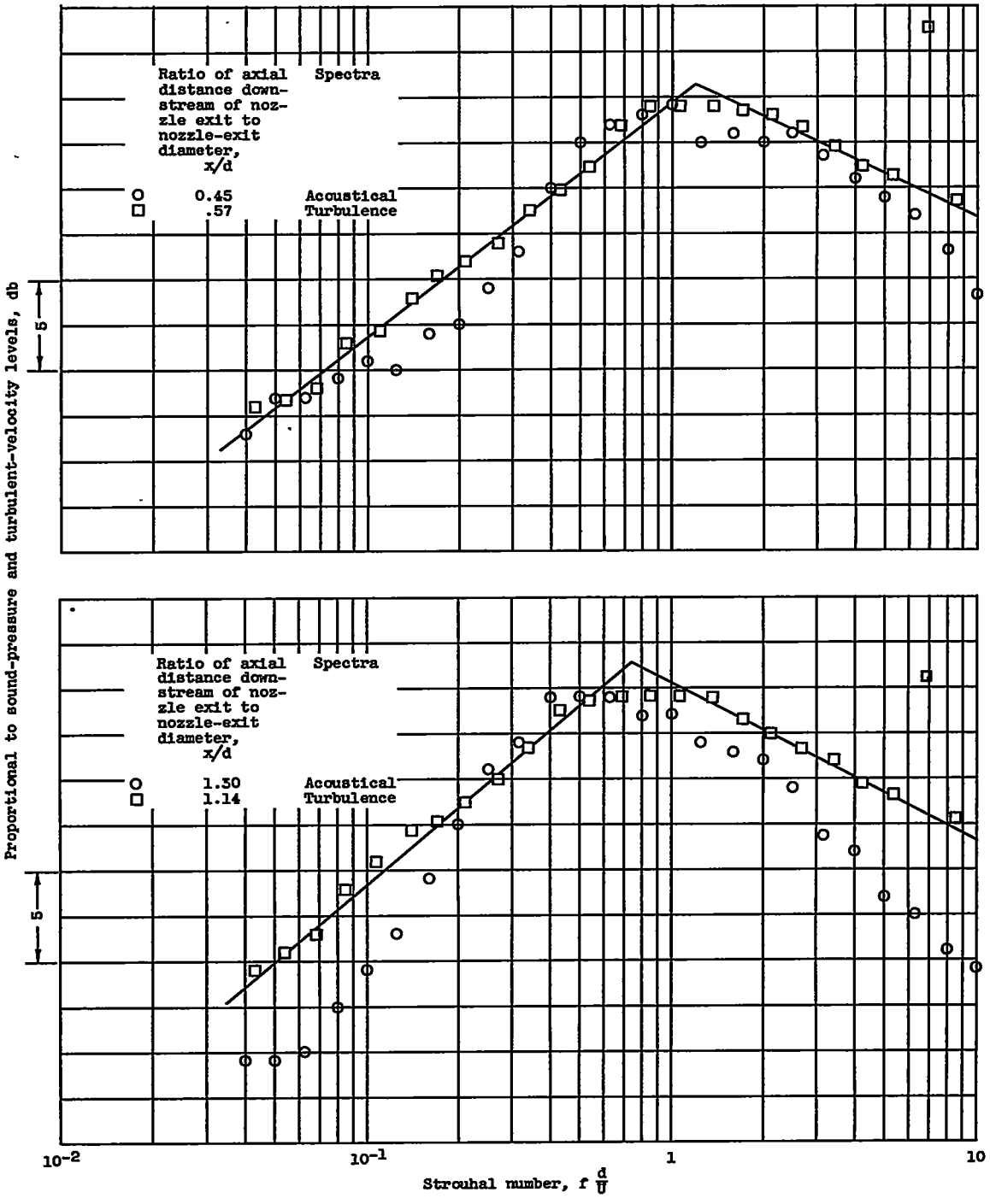

Figure 18. - Comparison of jet-engine accustical spectra along jet boundary with cold-air jet longitudinal turbulent-velocity spectra at 1 jet radius and same dimensionless distance downstream. (U, jet velocity; f, frequency; d, nozzle-exit diameter.)

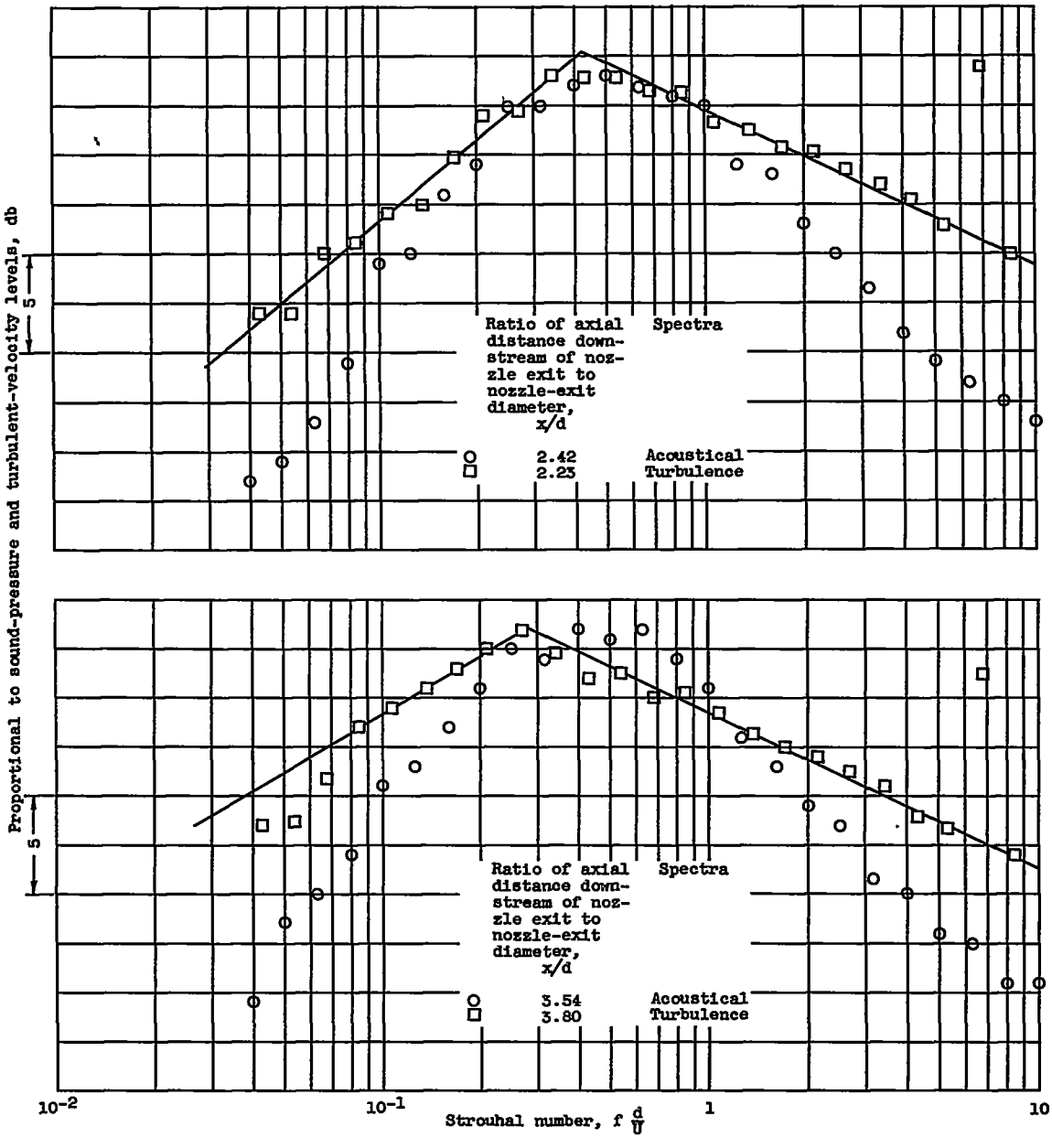

Figure 18. - Continued. Comparison of jet-engine acoustical spectra along jet boundary with cold-air jet longitudinal turbulent-velocity spectra at 1 jet radius and same dimensionless distance downstream. (U, jet velocity; f, frequency; d, nozzle-exit diameter.)

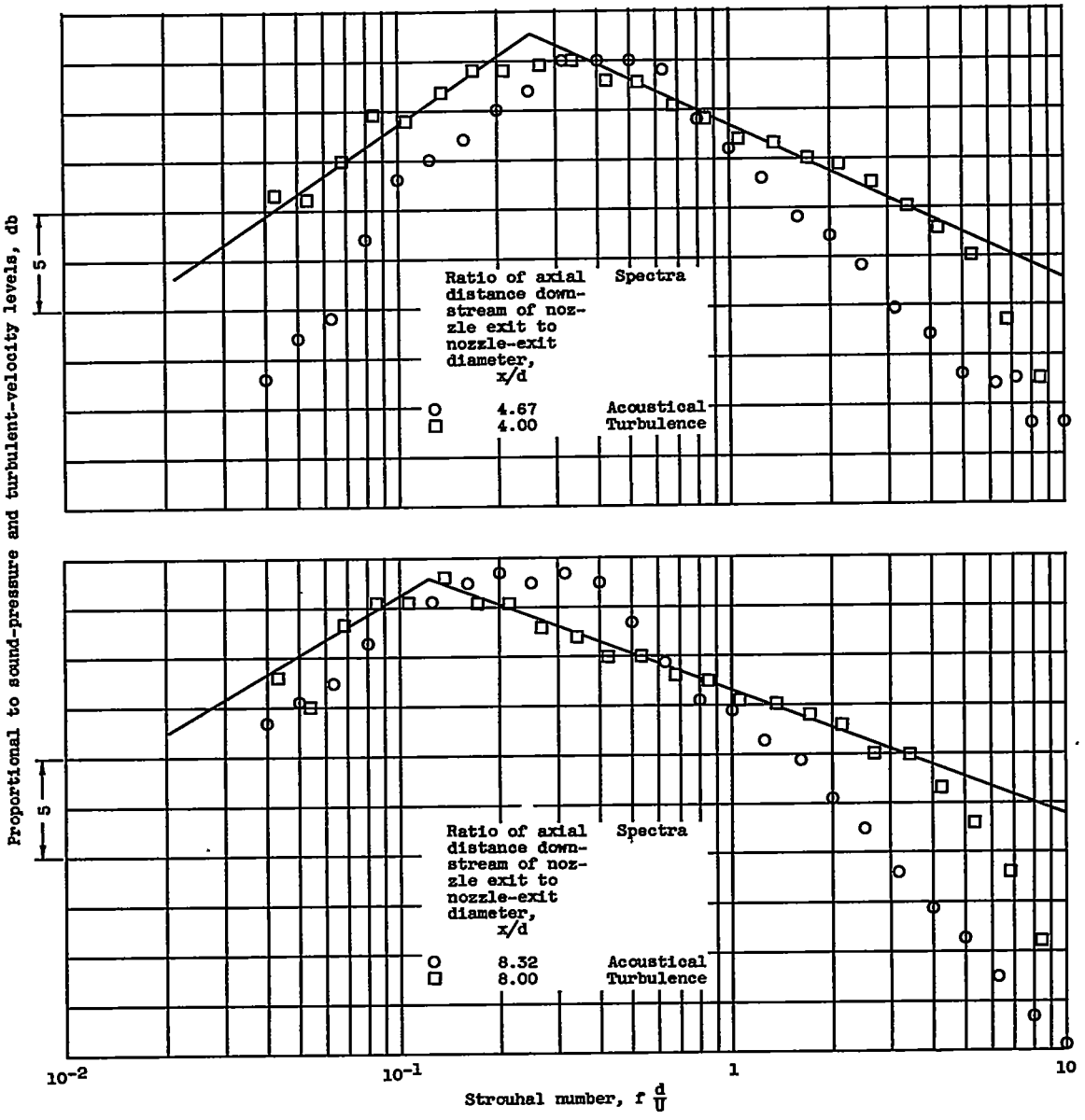

Figure 18. - Continued. Comparison of jet-engine acoustical spectra along jet boundary with cold-air jet longitudinal turbulent-velocity spectra at 1 jet radius and same dimensionless distance downstream. (U, jet velocity; f, frequency; d, nozzle-exit diameter.)

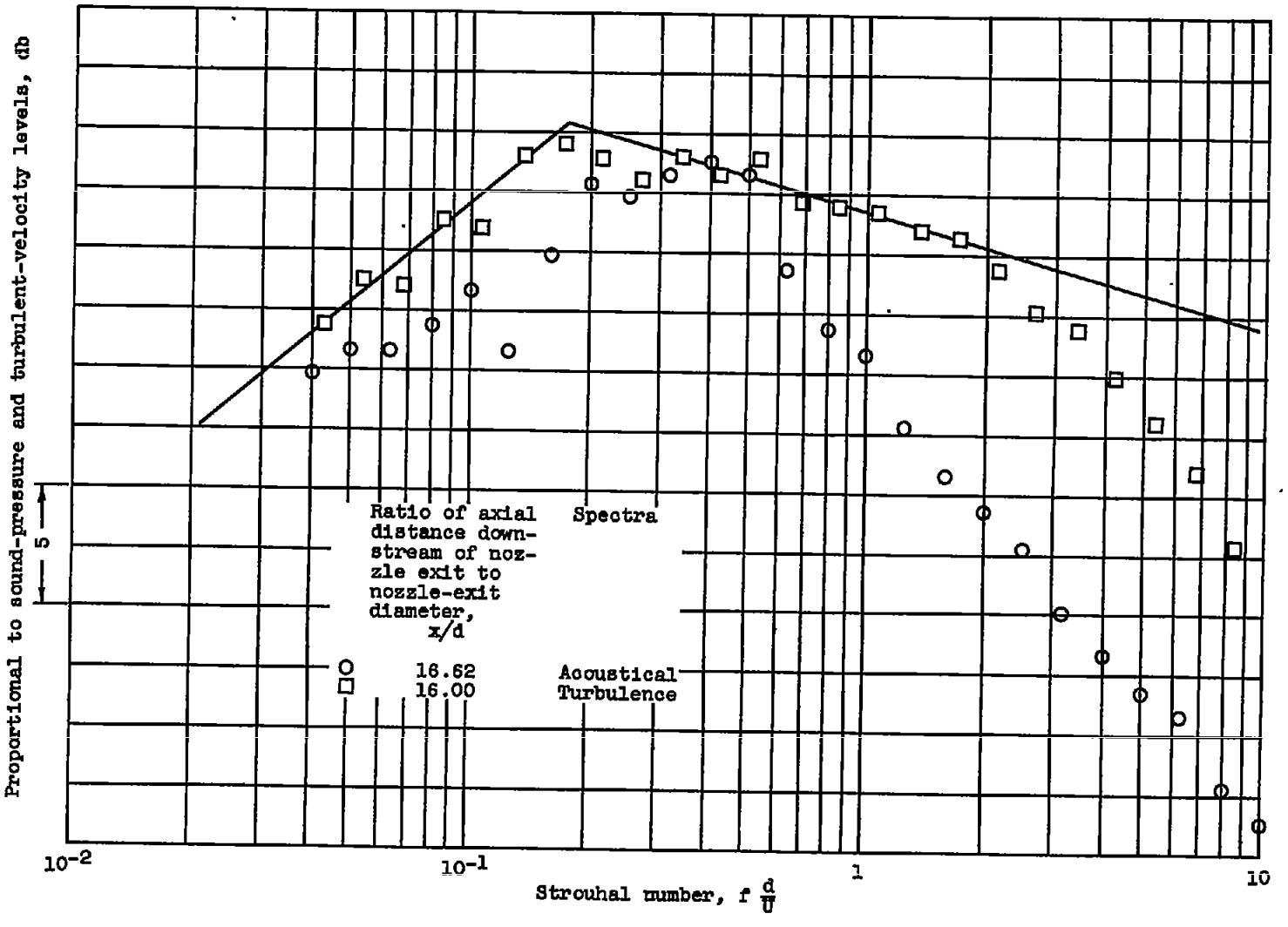

Figure 18. - Concluded. Comparison of jet-engine acoustical spectra along jet boundary with cold-air jet longitudinal turbulent-velocity spectra at 1 jet radius and same dimensionless distance downstream. (U, jet velocity; f, frequency; d, nozzle-exit diameter.)